

The large-scale structure of the universe: Turbulence, intermittency, structures in a self-gravitating medium

S. F. Shandarin

*Institute for Physical Problems, Academy of Sciences of the USSR, 117 334 Moscow, Union of Soviet Socialist Republics
and Max-Planck-Institut für Physik und Astrophysik, Institut für Astrophysik, 8046 Garching bei München, Federal Republic of Germany*

Ya. B. Zeldovich*

Institute for Physical Problems, Academy of Sciences of the USSR, 117 334 Moscow, Union of Soviet Socialist Republics

The density distribution arising at the nonlinear stage of gravitational instability is similar to intermittency phenomena in acoustic turbulence. Initially small-amplitude density fluctuations of Gaussian type transform into thin dense pancakes, filaments, and compact clumps of matter. It is perhaps surprising that the motion of self-gravitating matter in the expanding universe is like that of noninteracting matter moving by inertia. A similar process is the distribution of light reflected or refracted from rippled water. The similarity of gravitational instability to acoustic turbulence is highlighted by the fact that late nonlinear stages of density perturbation growth can be described by the Burgers equation, which is well known in the theory of turbulence. The phenomena discussed in this article are closely related to the problem of the formation of large-scale structure of the universe, which is also discussed.

CONTENTS

I. Introduction	185	VI. Gravitational Sticking	207
II. One-Dimensional Motion of Nongravitating Matter	189	VII. The Late Stage of Nonlinear Gravitational Instability	208
A. Early nonlinear stage	189	VIII. Numerical Simulations	210
1. Zero-temperature collisionless matter	189	IX. Statistical Analysis of Large-Scale Structures	212
2. The role of velocity dispersion	192	A. Correlation analysis	213
3. Gas	193	B. Percolation analysis	214
4. Sticky dust	194	X. Summary	216
B. Late nonlinear stage	194	Acknowledgments	217
1. Collisionless medium	194	References	217
2. Gas	195		
3. Sticky dust	195		
III. Two- and Three-Dimensional Motion of Nongravitational Matter	197		
A. Collisionless medium	197		
B. Similarity with geometric optics	198		
C. Motion as mapping and catastrophe theory	199		
D. Topology of the regions of multistream flows	200		
IV. Gravitating Matter. Cosmology	202		
A. Dark matter in the universe	202		
B. Linear gravitational instability	203		
C. Hot and cold dark matter	204		
D. Equality epoch	204		
E. Spectrum of density fluctuations at $z < z_{eq}$	205		
F. Decoupling epoch	205		
V. Approximate Solution of Nonlinear Gravitational Instability	206		

I. INTRODUCTION

Let us imagine a cold, homogeneous medium in the absence of gravitation with a given smooth velocity distribution at an initial time $t=0$. Its motion is easily described in Lagrangian coordinates. The actual position (i.e., Eulerian coordinates \mathbf{x}) of a particular particle is given as a function of its initial (Lagrangian) coordinates \mathbf{q} and time t by

$$\mathbf{x}(t, \mathbf{q}) = \mathbf{q} + t \cdot \mathbf{v}(\mathbf{q}), \quad (1.1)$$

where $\mathbf{v}(\mathbf{q})$ is the initial velocity. The simple form of Eq. (1.1), which is linear in t , implies that each particle moves with constant velocity. This is because the matter is cold, so that its pressure and viscosity are negligible, and because no forces are included.

The analysis of this trivial situation becomes more complicated if one assumes (as we shall) that $\mathbf{v}(\mathbf{q})$ is not necessarily a particular (smooth) function, but may be given by a random statistical distribution.

The motion according to Eq. (1.1) gives rise to intersections of trajectories and formation of regions of high (or even infinite) density.

In the case of an ordinary gas subject to collisions, the motion leads to the formation of shock waves and various phenomena (such as heat conduction) related to the subsequent heating of the gas.

Both processes are relevant to the formation of large-

*Deceased. The Russian version of this review was finished in the summer of 1987. By the tragic death of Ya. B. Zeldovich on December 2, 1987, about four-fifths of the paper had been translated into English. Professor Zeldovich would have been 75 years old on March 8, 1989 and was vivid and creative until his last day. The theory of the structure of the universe was one of his favorite subjects, to which he made many note-worthy contributions over the last 20 years.

scale structure in the universe that results from the presence of at least two distinct mass components. One of them is supposed to be collisionless nonrelativistic matter composed of weakly interacting massive particles such as neutrinos, axions, photinos, etc. It is generally assumed to comprise about 90% (or even more) of the total mass of the universe. The other component is an ordinary gas of baryons amounting to less than about 10% of the total mass.

In a collisionless medium of weakly interacting particles, multistream configurations may form. This means that at a point with Eulerian coordinates \mathbf{x} there are particles that have arrived from different points in Lagrangian space with coordinates $\mathbf{q}_1, \mathbf{q}_2, \dots, \mathbf{q}_n$. These particles have different velocities $\mathbf{v}_1, \mathbf{v}_2, \dots, \mathbf{v}_n$, and this situation differs from the initial state at $t=0$, in which the medium is cold (zero temperature) and all particles having the same coordinates also have the same velocities $\mathbf{v}(\mathbf{q})$.

The formation of multistream configurations and the analysis of their properties is an excellent starting point for the study of catastrophe theory, as developed by René Thom and Vladimir Arnold. It is a grave omission that the *Reviews of Modern Physics* has never given space to this subject. However, there are others more expert in catastrophe theory than the present authors; it has, moreover, received ample coverage outside the pages of *Reviews of Modern Physics*. In this paper we are concerned with catastrophe theory only from the point of view of mechanical problems. There is no sociology, no psychology, etc.

Here we shall give detailed analysis of density inhomogeneity structures including both local and global properties arising in potential motions by pure inertia as well as under self-gravity of moving matter.

Let us return to the particular example of freely-moving collisionless particles and discuss the late stage when most of the particles have experienced trajectory intersections. The ultimate fate of the system at infinite time is predetermined. If the initial velocity field satisfies natural statistical properties, then the final state will be a Maxwellian thermal equilibrium velocity distribution with normal coarse-grained fluctuations in the density and other common statistical properties.

However, there is an intermediate nontrivial stage: After the birth of local singularities (we shall refer to a continuous surface or a continuous curve with singularities on it as a caustic), regions of high density grow and form a peculiar structure known by various names—“cellular structure,” “sponge,” “foam,” etc. The main feature of this structure is the existence of comparatively thin layers and filaments of high density that separate large regions of low density. In the layers and filaments the flow consists of many streams, whereas in the low-density regions there is only one stream. Later all structure of this kind is destroyed.

In this paper we discuss this intermediate-stage structure. This study began as a treatment of a purely cosmological problem, that of large scale structure formation, and we shall discuss cosmology in later parts of the pa-

per. For now, we mention just two points: First, the kind of structure in question may have been found in the spatial distribution of galaxies (Fig. 1). Second, it is very probable that most of the mass in the universe is composed of weakly interacting massive particles, which form a collisionless medium filling up space.

But we must explain the use of the term “turbulence” in the title. The classical concept of turbulence emerged in connection with problems of fluid mechanics dealing with the motion of an incompressible liquid. The condition of constant density leads to divergence-free flow. The velocity can be described as the curl of a vector potential $\mathbf{v} = \text{curl } \mathbf{A}$.

Reynolds’s astonishing observation performed more than a century ago concerns the formation of irregular eddies having intermediate sizes between large-scale boundaries of the flow and small scales dominated by viscosity.

Let us consider the evolution of the flow (instead of more familiar stationary flows). Starting from an initially smooth, laminar flow, one obtains finally (formally in infinite time) fluid at rest but at a somewhat higher temperature. However, the intermediate behavior of the liquid depends on the Reynolds number $\text{Re} = Lv/\nu$, where L and v are, respectively, length and velocity scales of the flow, and ν is the kinematic viscosity of the liquid. If Re is less than some critical value, the flow remains laminar for all time, but if Re is greater than this critical value, the flow becomes turbulent, and only later after damping has occurred will it again become laminar before dying completely.

One of the authors remembers that about thirty years ago the usual joke was to ask someone what turbulence is. In 99% of all cases, the answer was given by some rotational hand waving instead of articulate words. Now a highbrow theoretician would give an answer in terms like “stochasticity,” “strange attractor,” “intermittency,” etc. Moreover, at present one can speak about turbulence in systems with a few degrees of freedom, in any case greater than 1.5 (see, for example, Eckmann, 1981; Ott, 1981). In mechanical problems, every degree of freedom is associated with one differential equation of second order or two equations of first order. Stochasticity and strange attractors arise in systems of three nonlinear equations of first order, which gives rise to a strange fractional number for degrees of freedom $1.5 = \frac{3}{2}$. From this point of view, the approach to the evolution of density inhomogeneities developed in this paper is undoubtedly the restoration of the classical Reynolds viewpoint on turbulence in a continuous medium. However, the structures arising in classical incompressible liquid turbulence are not as clear as in our case of potential motions of a collisionless medium. It is necessary to stress the essentially nonlinear character of the phenomena in question, which cannot be analyzed with spectral Fourier methods.

To make this clear, let us consider the hydrodynamic flow of a fluid with small pressure gradients and viscosity. Strictly speaking, one needs to have small deviations of density, which will occur if the motion is quite subson-

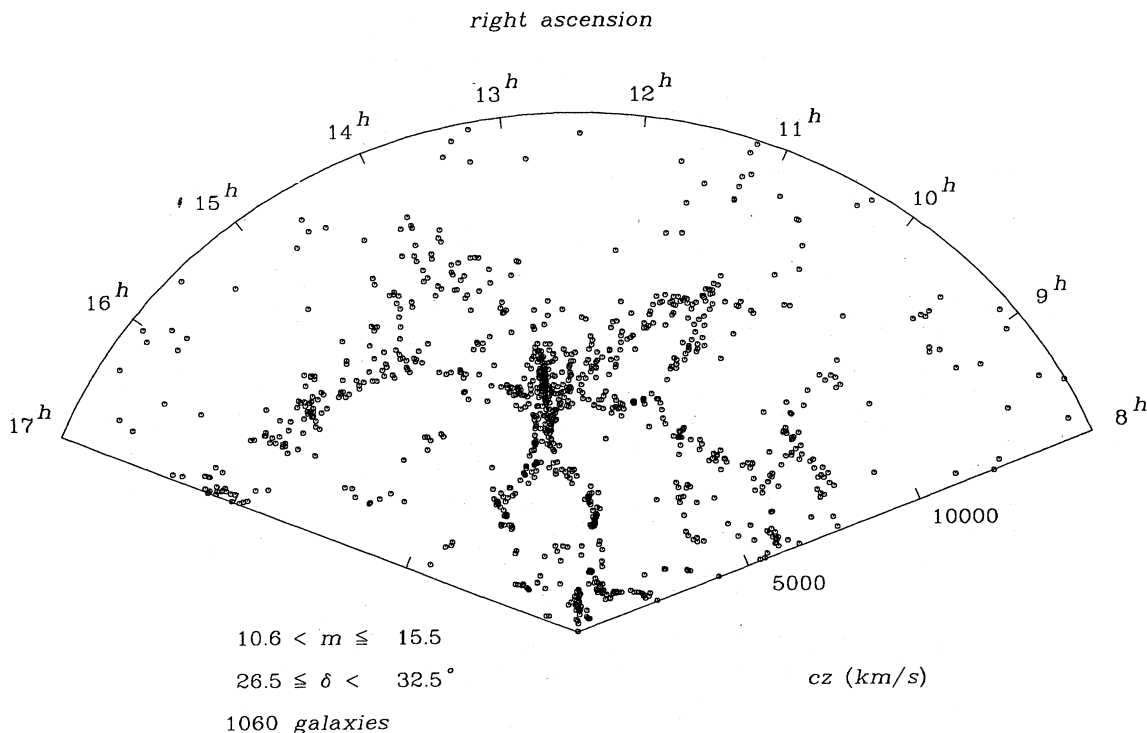


FIG. 1. The distribution of galaxies in a thin slice with $8^h \leq \alpha \leq 17^h$ and $26.5 \leq \delta \leq 32.5$, where α (right ascension) and δ (declination) are spherical coordinates (de Lapparent *et al.*, 1986). The positions of 1060 galaxies with $m_B \leq 15.5$ and $v \leq 15000 \text{ km s}^{-1}$ are indicated. The scale shows the velocities of the galaxies, and their distances can be estimated assuming that the velocity and the distance of a galaxy are related according to Hubble's law, $v = H_0 r$ ($H_0 = 50 h_{50} \text{ km s}^{-1} \text{ Mpc}^{-1}$).

ic, $M \ll 1$, where $M = v/c_s$ is the Mach number.

If the amplitude of the initial velocity distribution is small, then the nonlinear terms in the gas dynamic equations are also small, and one can use the Fourier method or normal mode analysis. Every mode will damp out due to viscosity. Short waves are damped more quickly, long waves survive longer. As a result of damping, the velocity field gets smoother. The final result is obvious: the fluid is at rest in a state of thermal equilibrium (if even a small amount of heat conduction is present) at some new higher temperature, but nothing particularly interesting occurs in between.

Qualitatively new behavior of flows in the case of large initial velocity is associated with the nonlinear character of the gas dynamic equations. The nonlinearity couples different modes. As a result, even with smooth initial conditions, higher harmonics arise. Both the velocity and the density distributions become steeper, at least in some places, constituting a radical departure from the linear regime.

Fourier analysis including nonlinear effects in higher orders shows the general trend of the evolution. However, it loses the ability to describe the process quantitatively. The main reason is that in the nonlinear regime the distribution of phases of different modes ceases to be statistically independent, even if it was at the linear stage. At this stage, the Fourier spectrum is the unique statisti-

cal measure neither of velocity nor of the spatial density distribution. The spectra of density fields with singularities (i.e., caustics) possess an abundant short-wave component. However, the phases of the short waves are not statistically independent, with the result that Fourier analysis loses most of its appeal. Thus one is forced to return to characteristics that were used by Riemann for analysis of the formation of shock waves from large-amplitude acoustic waves. Particle trajectories used in the Lagrangian approach are the characteristics in pressureless gas dynamics.

Let us return to turbulence in an incompressible liquid. It is amazing that the turbulence discovered in experiments conducted more than a century ago remains one of the most difficult phenomena to explain, in spite of the fact that much has been done in an effort to understand it.

One approach to the problem is a drastic reduction in the number of degrees of freedom. Generalized coordinates are introduced that represent the amplitudes of a few spatial movement patterns (normal or even "abnormal" modes). As a result one can obtain a system of a few nonlinear ordinary differential equations instead of the partial equations of hydrodynamics. As we have already mentioned, a system of three nonlinear equations of first order (1.5 degrees of freedom) can reproduce some features of turbulence, e.g., stochastic aperiodic motion.

This phenomenon, unexpected up to the second half of the twentieth century, has been called a "strange attractor." (It certainly attracts many theoreticians.) But the spatial patterns of turbulence are lost in the approach.

In this paper, spatial patterns are considered, though at the cost of a considerable simplification of the problem. We begin with a simple system of noninteracting particles, for which the nonlinear character of Eulerian description is significant. Here nonstationary aspects of the evolution of density inhomogeneities are considered assuming specific initial conditions. Thus periodic solutions have been excluded from the very beginning. All these assumptions have been made in order to obtain clear and definite statements concerning the spatial patterns arising in the motion. The formation of a whole spectrum of intermediate scales is the property that unifies the motion of a collisionless medium with Reynolds turbulence of an incompressible liquid. The underlying hope is that perhaps the spatial patterns in our case will provide some inspiration in the study of turbulent patterns in ordinary liquids.

The last point to discuss here is gravitation. One cannot overestimate its importance in dealing with cosmological applications. The problem of force-free motion stated at the beginning is related to the cosmological problem only as the first, simplest step. In fact, small density fluctuations grow in an expanding universe under the action of gravity. This process is called gravitational instability.

It turns out that, at a rather late stage of the expansion of the universe (which will be defined later), the matter in the universe can be described as cold dust moving under the action of gravity alone. At this stage, the motion of each particle can be approximately described by a simple law (Zeldovich, 1970),

$$\mathbf{r}(t, \mathbf{q}) = a(t) [\mathbf{q} - b(t) \mathbf{s}(\mathbf{q})], \quad (1.2)$$

where, as in Eq. (1.1), \mathbf{r} and \mathbf{q} are Eulerian and Lagrangian coordinates, respectively, $a(t)$ is the cosmological expansion factor, $b(t)$ is the growth rate of linear density fluctuations in the expanding universe, and $\mathbf{s}(\mathbf{q})$, which can be expressed as the gradient of a potential $\mathbf{s}(\mathbf{q}) = \nabla \Phi(\mathbf{q})$, represents the spatial perturbation. The first product on the right-hand side, $a(t)\mathbf{q}$, is the unperturbed position. The growth function $b(t)$ depends also on the dimensionless mean mass density of the universe $\Omega = \bar{\rho}/\rho_{cr}$, but in a flat matter-dominated universe ($\Omega = 1$), $b(t) \propto a(t)$. Unless the density perturbations are nonlinear, $\delta\rho/\rho \propto \nabla \mathbf{s}(\mathbf{q}) \propto \nabla^2 \Phi(\mathbf{q})$. The sign of the second term in Eq. (1.2) is chosen to be negative by convention in cosmology. Making a simple transformation

$$\mathbf{x} = \mathbf{r}/a(t), \quad \tau = b(t), \quad \mathbf{v}(\mathbf{q}) = -\mathbf{s}(\mathbf{q}), \quad (1.3)$$

one easily obtains instead of Eq. (1.2)

$$\mathbf{x} = \mathbf{q} + \tau \cdot \mathbf{v}(\mathbf{q}). \quad (1.4)$$

Since Eq. (1.4) is of the same form as (1.1), some features of the motion of noninteracting matter in accordance

with (1.1) persist in the case of gravitating systems. Moreover, since the accelerations in gravitating systems are caused by gradients of the gravitational potential, one can assume that the velocity field is of the potential type

$$\mathbf{v} = \nabla \Phi.$$

If rotations were initially present, they would be strongly damped due to the expansion. This makes the analysis more definite.

The simple formula (1.2), mimicking the motion of a noninteracting medium, describes the motion of a gravitating medium up until the stage of caustic formation. In fact, one can reasonably speculate that the singularities arising in both cases are of the same type. But the motion of a gravitating medium soon becomes quite different from the prediction of (1.2). As a result, the final states of these two media are quite different. It is well known that a self-gravitating medium cannot achieve thermodynamic equilibrium in an infinite universe. The spectre of the thermal death of the universe, often mentioned in the nineteenth century, no longer haunts us. In the twentieth century it has given place to the "Dracula" of collapsing black holes.

What is of practical importance for cosmology is the speculation that the observed large-scale structure of the universe (Fig. 1) (de Lapparent *et al.*, 1986; Postman *et al.*, 1986; Tago *et al.*, 1986) represents an intermediate stage, resulting from the gravitational instability of a slightly perturbed density distribution. Depending on the spectrum of the density fluctuations at the linear stage ($\delta\rho/\rho \ll 1$), the formation of structure may proceed mainly in one of two ways: the first, known as the "bottom-up" scenario, predicts the sequence galaxies—clusters of galaxies—superclusters. The other, known as the "top-down" scenario, predicts the opposite sequence. We shall discuss these scenarios in more detail later, but at present we wish to stress that the kind of scenario depends on the kind of dark matter. The top-down scenario takes place in a universe dominated by hot dark matter composed of massive neutrinos with a rest mass of about 30 eV (assuming they have such a mass) (Doroshkevich *et al.*, 1981). The bottom-up scenario takes place in a universe dominated by cold dark matter made of axions, photinos, or other exotic particles invented by particle physics theorists, but not yet observed in the laboratory.

In any case, one can observe the peculiar large-scale structure in the universe because the universe is neither too young (in which case it would not have had enough time to develop) nor too old (because this structure does exist at present).

Let us put this in terms of the anthropic principle: Mankind could not have been created very early before the formation of galaxies and stars, which need time for density perturbation growth. But life emerged almost as early as possible (on the cosmological scale of time) after the birth of the sun, one of the typical second generation stars. Later highly anisotropic superclusters (Fig. 1) will be destroyed by gravitational forces that collect most of

the galaxies into large clumps of much less anisotropic shapes. Thus the only stage at which this structure can be observed is its present, intermediate stage, when both structure and observers exist.

Returning to the topic of our review let us formulate the problems we wish to address and briefly repeat the contents of this paper: In modern cosmology there are two fundamental problems. The first is to understand the physical nature of dark matter, and the second is to explain the type, spectrum, and amplitude of primordial density fluctuations, which finally result in galaxies and other large-scale structures. Both problems are closely connected with our understanding of the nonlinear evolution of density inhomogeneities.

In this context, among the most interesting observable structures in the universe are superclusters of galaxies. (For a review of supercluster properties see Oort, 1983.) The superclusters of galaxies and voids in between are the largest density inhomogeneities, having sizes of more than 30 Mpc ($\sim 10^{26}$ cm) (1 Mpc = 10^6 pc $\approx 3 \times 10^{24}$ cm). Superclusters are nonlinear ($\delta\rho/\rho > 1$) but still nonrelaxed systems preserving some information about the spectrum of initial (i.e., linear) density perturbations. In addition, they are the obvious place to look for the influence of dark matter, which is most important on large scales.

We shall discuss the formation of large-scale structure based on gravitational instability. This phenomenon, as well as its importance for cosmology, was already understood by Newton. However, to be fair we ought to mention that, since Newton's time, other mechanisms of structure formation have been suggested.

One of these invokes the hypothesis of cosmic strings (not be confused with superstrings), which represent topological distortions of space-time possessing a high energy density (Kibble, 1976; Zeldovich, 1980; Vilenkin, 1981, 1985; Rees, 1986; Turok, 1986). Actually, in the model of structure formation based on this hypothesis, the phenomenon of gravitational instability is also used. The essential difference of this model from the one we shall discuss is the non-Gaussian character of the initial perturbations.

Another model is based upon the hypothesis that collective supernova explosions may provide an enormous amount of energy (Ostriker and Cowie, 1981; Carr and Ikeuchi, 1985; Weinberg *et al.*, 1988). In this model, thermal and gas dynamic phenomena play a much more important role than they do in the traditional instability picture.

Without criticizing the cosmic string and explosion scenarios, we must state that, to our mind, the gravitational instability model is better developed at present, and—what seems even more important—it is based on initial conditions whose statistics can be specified uniquely.

An additional motivation for discussing nonlinear gravitational instability is its similarity to turbulence and different synergetic problems that have recently been clarified. One can characterize the phenomena discussed

in this paper as a whole as the “physics of gravitating media.” However, we should stress that they have little in common with those discussed in the well-known book by Friedman and Polyachenko (1984), since in our review we shall consider neither spiral galaxy structures nor other related problems.

We begin with a detailed discussion of the nonlinear phenomena occurring in noninteracting media, where every fluid particle moves owing to inertia, starting from the simplest one-dimensional motion. Two- and three-dimensional systems are then considered. It turns out that, even in this oversimplified approach, nontrivial effects arise like caustics, peculiar cellular structures, and so on. What is even less trivial is that similar structures arise from the growth of density perturbations due to gravitational instability in the expanding universe. We discuss this and conclude the review by application of these phenomena to the observed large-scale structure of the universe.

II. ONE-DIMENSIONAL MOTION OF NONGRAVITATING MATTER

In this section we shall study the motion of matter without any interaction at all. As we shall see, this process is an excellent starting point for an analysis of the more complicated process of the growth of density perturbations under the action of gravitational instability.

An additional simplification is gained by considering one-dimensional flow. As will be shown later, locally one-dimensional motion is generic at the beginning of the nonlinear stage in real two- and three-dimensional flows, when caustics (i.e., surfaces of infinite density) and shock fronts form. As a result, the first objects formed at the nonlinear stage are “pancakes.” Some of the general properties of pancakes can be analyzed in the one-dimensional case.

A. Early nonlinear stage

1. Zero-temperature collisionless matter

The simplest problem we begin with is the one-dimensional motion of a zero-temperature, collisionless, continuous medium.

Suppose that at the initial time $t=0$ the density of matter is homogeneous, i.e., $\rho(x,0)=\rho_0$, and let $v(x,0)=v_0(q)$ be the initial velocity field. Here q can also be interpreted as a Lagrangian coordinate: $x=q$ at $t=0$.

In this case one can easily find the position of every particle in terms of the Eulerian coordinates at any time t ,

$$x(q,t)=q+t \cdot v_0(q). \quad (2.1)$$

At $t>0$, the density of matter becomes inhomogeneous. Using the mass-conservation law $\rho(x,t)dx=\rho_0dq$,

one can calculate the distribution of density as a function of the Lagrangian coordinate q ,

$$\rho(q, t) = \frac{\rho_0}{1 + t \cdot \alpha(q)}, \tag{2.2}$$

where $\alpha(q) = dv_0/dq$. To find the true density distribution in Eulerian space, one needs to invert Eq. (2.1) to obtain q . (In the general case, this cannot be done analytically.) An additional useful function is the initial velocity potential $\Phi_0(q) = \int v_0 dq$. In terms of the potential Φ_0 , $v_0 = d\Phi_0/dq$, $\alpha(q) = d^2\Phi_0/dq^2$, and $\rho = \rho_0 / (1 + t d^2\Phi_0/dq^2)$.

At the linear stage [at small t while $|t \cdot \alpha(q)| \ll 1$] Eq. (2.2) for the density can be simplified to

$$\rho(q, t) \approx \rho_0 [1 - t \cdot \alpha(q)]. \tag{2.3}$$

Incidentally at this stage $x \approx q$, and Eq. (2.3) also gives the real distribution of density in Eulerian space. Thus the function $\alpha(q) = dv_0/dq = d^2\Phi_0/dq^2$ reproduces the density distribution at the linear stage.

In the course of time, the amplitude of the density perturbations grows and the linear equation (2.3) becomes invalid. One must use the general equation (2.2), which predicts that at time

$$t(q) = -1/\alpha(q) \tag{2.4}$$

the density at the point with Lagrangian coordinates q becomes infinite. In corresponding points of Eulerian space there are caustics.

One can easily see from Eq. (2.4) that the first singularities arise locally at the negative minima of $\alpha(q)$. Immediately after that two neighboring points achieve infinite density and become the boundaries of regions with three-stream flows (Figs. 2 and 3). These events are evidently consequences of the motion of particles, in that the velocities are constant in time but varying from point to point. After some time rapidly moving particles begin to catch up and outstrip the slow ones.

In the vicinity of a negative minimum of $\alpha(q)$ (in Lagrangian space), two neighboring points exchange their positions for the first time. As a result, a density singularity arises in Eulerian space at the corresponding time (Fig. 2).

As a mechanical problem, the calculation of the density distribution in the vicinity of the singularity is fully determined by the initial conditions, i.e., the initial velocity distribution $v_0(q)$. What is particularly important here and later is that we consider generic velocity fields only. A typical and practically interesting example of such a field is the velocity distribution given by a finite or infinite trigonometric sum,

$$v_0(q) = \sum_{k=1}^{N_k} V_k \cos(kq + \varphi_k), \tag{2.5}$$

where V_k and φ_k are random, statistically independent numbers, and N_k can be infinite in the case of a convergent series.

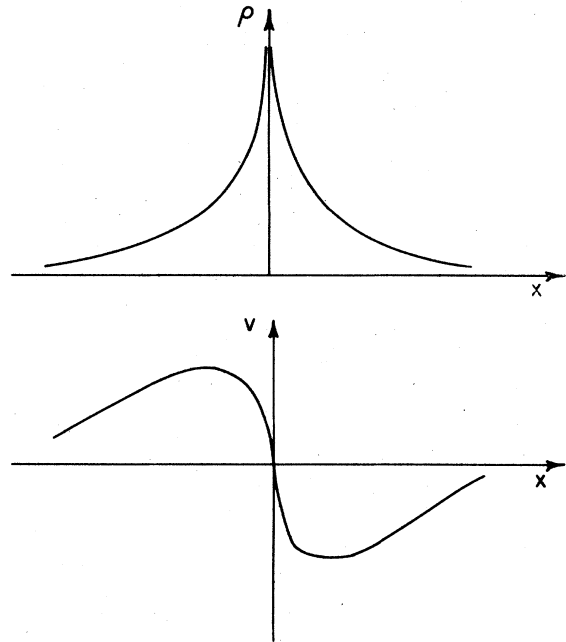


FIG. 2. The formation of a pancake begins with the development of a singularity in the density distribution. It has a particular form $\rho \propto |x|^{-2/3}$ in the vicinity of $x=0$ and is schematically illustrated in panel (a). Exactly at the time of the singularity formation, the velocity field develops a vertical tangent at the position of the singularity. This is schematically illustrated in panel (b). At $x=0$, $dv/dx = \infty$.

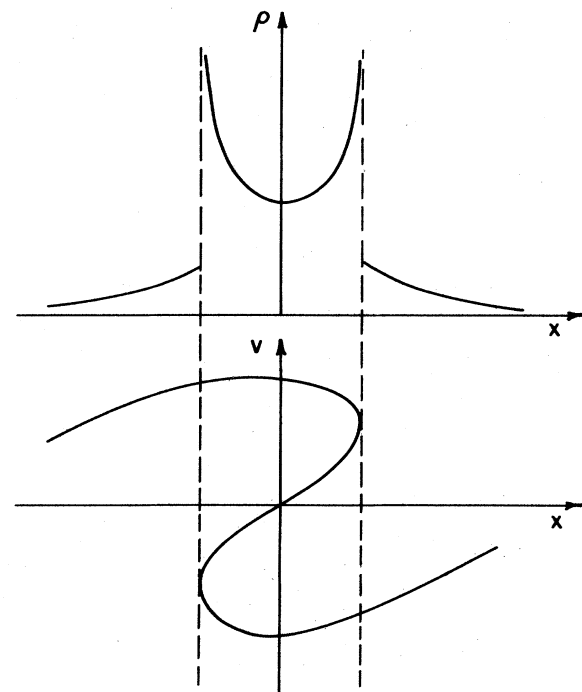


FIG. 3. Density and velocity distribution a short time after pancake formation. The boundaries of the three-stream flow region are indicated by dashed lines. Inside the three-stream region in the vicinity of the border $\rho \propto |x - x_s|^{-1/2}$.

To analyze the structure of the singularity, one has to expand $v_0(q)$ in a Taylor series in the vicinity of the minima of $\alpha(q)$. If for convenience we put the origin of coordinates at the point in question, we obtain in the generic case

$$v_0(q) = -\alpha_0 \left[q - \frac{1}{l_0^2} q^3 + \dots \right], \tag{2.6}$$

where $-\alpha_0 = \alpha(0)$ and where l_0 is the spatial scale of the velocity field; the term of second order in q is absent, since we are considering a minimum point of $\alpha(q)$.

Using Eqs. (2.1) and (2.2), one easily obtains for the density distribution at $t_0 = 1/\alpha_0$ (Fig. 2)

$$\rho(t_0, x) = \frac{\rho_0}{3} \left[\frac{x}{l_0} \right]^{-2/3}, \quad |x| \ll l_0, \tag{2.7}$$

where ρ_0 is the initial density. Thus in the generic case the first singularity is of the power-law kind. By the way, the mass in the immediate vicinity of the singularity is small,

$$\Delta m = \int_{-\epsilon}^{\epsilon} \rho(x) dx \propto \epsilon^{1/3}.$$

This singularity is instantaneous. Immediately after forming it disappears, and two singularities of another kind arise in its place. The region of three-stream flow emerges in between (Fig. 3).

Shortly after, at $t_1 = t_0 + \Delta t$, the Lagrangian and Eulerian coordinates of the singularities are, respectively,

$$\begin{aligned} q_s &= \pm \frac{l_0}{\sqrt{3}} \left[\frac{\Delta t}{t_0} \right]^{1/2}, \\ x_s &= -2 \frac{q_s^3}{l_0^2} = \pm \frac{2}{3} \frac{l_0}{\sqrt{3}} \left[\frac{\Delta t}{t_0} \right]^{3/2}. \end{aligned} \tag{2.8}$$

At any $-x_s < x < x_s$, the equation $x = q + t_1 v_0(q)$ has three solutions, q_1, q_2, q_3 , implying that at every point x there are three particles having different velocities (Fig. 3). The mass of the three-stream flow region increases proportionally to $(\Delta t/t_0)^{1/2}$, and therefore the mean density of the region is

$$\bar{\rho}_3 = 3\rho_0 \left[\frac{\Delta t}{t_0} \right]^{-1}. \tag{2.9}$$

A simple calculation yields the approximate density distribution near the singularities in the three-stream flow region

$$\rho(t_0 + \Delta t, \Delta x) = \rho_0 \left[\frac{2}{27} \right]^{1/6} \left[\frac{x_s}{l_0} \right]^{-2/3} \left[\frac{\Delta x}{x_s} \right]^{-1/2}, \tag{2.10}$$

where $\Delta x = |x - x_s|$ is the distance from the nearest singular point. This equation actually represents the sum of two streams having singularities at x_s ; the influence of the third stream, having finite density, is small near the

singularities. This kind of singularity is even weaker than the previous one, and the mass in its vicinity is

$$\Delta m = \int_{x_s - \epsilon}^{x_s} \rho(x) dx \propto \epsilon^{1/2}.$$

Equation (2.10) can be used only for a short time after the origination of a three-stream flow region. About a given point, the velocity can be expanded in the form

$$v(q) = -\alpha_1 \left[q - \frac{1}{l_1} q^2 + \dots \right], \tag{2.11}$$

where l_1 is a typical space scale of the velocity field. Generally speaking $l_1 \neq l_0$ [see Eq. (2.6)], but commonly $l_1 \sim l_0$.

Similar calculations give in the immediate vicinity of a singularity

$$\rho(t_0, x) = 2\rho_0 \left[\frac{x}{l_1} \right]^{-1/2}, \tag{2.12}$$

where $t_0 = 1/\alpha_1$ and x is the distance from the singularity. This equation again gives the sum of the densities due to two singular streams in the region of three-stream flow. Outside this region there is an infinite jump in the density distribution (Fig. 3).

It is instructive to illustrate the process of overshooting and the formation of three-stream flows by a three-dimensional phase diagram $v = v(x, t)$. In Fig. 4 the surface $v = v(x, t)$ is shown in the vicinity (both in space and time) of the point of overshooting. This phenomenon is well known in catastrophe theory as "Whitney's cusp." At $t < t_0$, the function $v = v(t, x)$ is single valued, but at $t > t_0$ it is triple valued.

The growth of density inhomogeneities at the nonlinear stage is connected with a rapid increase in the short-wavelength part of the spectrum, which reflects a steepening of the density distribution. However, at the

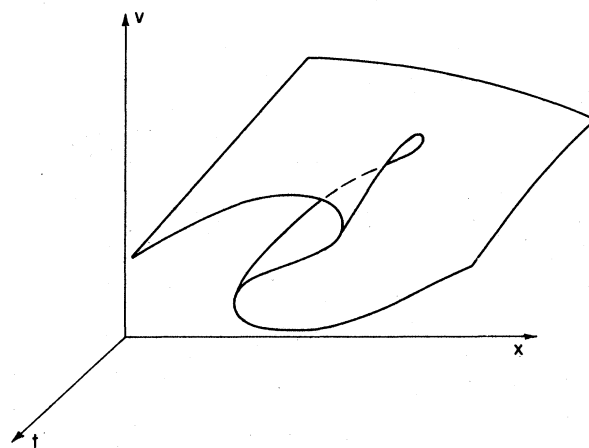


FIG. 4. Velocity distribution $v = v(x, t)$ in the shape of Whitney's cusp, in a region of pancake formation (in space-time coordinates).

final stage before the formation of singularities, the effect of coordination of phases is probably more important. The following example illustrates this statement.

Let the initial velocity distribution be of the simple sinusoidal type,

$$x(t, q) = q - t \sin q \quad (2.13)$$

At $t_0 = 1$ at the origin $x = 0$ the first singularity arises. At $t < t_0 = 1$ one can easily calculate the coefficients of the Fourier expansion,

$$\rho = \rho(t, x) = \rho_0 + \sum_{k=1}^{\infty} \rho_k(t) \cos kx,$$

$$\rho_k(t) = 2J_k(kt),$$

where $J_k(kt)$ are Bessel functions. The growth of the amplitudes is shown in Fig. 5. At $t \ll 1$, $\rho_k \propto t^k$, meaning that higher harmonics increase faster than lower ones; however, at any $t \leq 1$ they satisfy the inequality $\rho_{k+1}(t) < \rho_k(t)$. It is worth mentioning that at $t \sim 1$ the growth of the amplitude of the first wave even slows down compared with the extrapolation of the linear theory. Thus the formation of singularities is not caused by catastrophic growth of the amplitudes of short waves, as one might think, but rather due to coordination of phases.

The formation of singularities in the density distribution is a consequence of the two principal assumptions we have made. The medium was supposed to be (i) continuous and (ii) of zero temperature. Weakening either assumption eliminates the singularities. In a discrete system, the number of particles in the vicinity of singularities is proportional to the mass, i.e., finite. The influence of a small initial velocity dispersion is discussed in the next section.

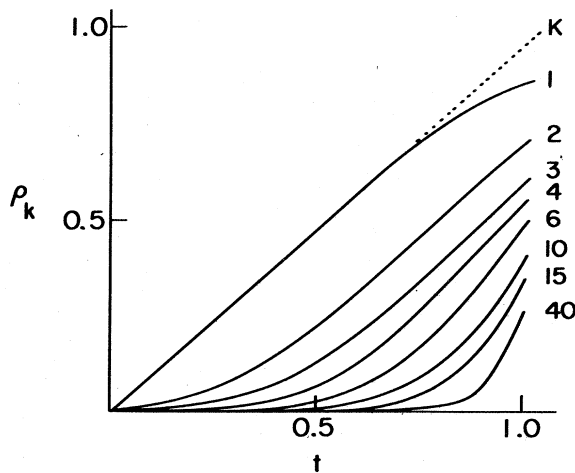


FIG. 5. Evolution of the amplitudes of the main and higher harmonics during the formation of a singularity in density distribution (Fig. 2). The numbers of the harmonics are indicated.

2. The role of velocity dispersion

Qualitatively it is easy to understand the effect of velocity dispersion on the density distribution by recognizing that calculating the density at a given point of Eulerian space (and at a given time) means geometrically mapping the phase curve $v = v(x, t)$ onto the x axis.

Singularities arise at those points where the curve $v(x, t)$ has a vertical tangent (Figs. 2 and 3). Thus density singularities occur due to the singular character of the initial phase density. An initial state with a thermal velocity dispersion is given by a strip of finite width in the phase space rather than a line. Its effective width is proportional to the velocity dispersion. Under a mapping, the phase strip produces no singularities.

Let us consider this question quantitatively (Shukurov, 1981; Zeldovich and Shandarin, 1982b; Kotok and Shandarin, 1987). In the initial state with constant density (except for thermal fluctuations), a smooth velocity field is given by $v = v(q)$ [Eq. (2.6)]. The thermal velocity distribution function is assumed to be independent of the spatial coordinates

$$f(t = 0, x, v_{th}) = f_0(v_{th}).$$

Now let us follow the motion of a stream with a given value of thermal velocity. Its initial density is $d\rho_0 = \rho_0 f_0(v_{th}) dv_{th}$. The motion of this stream does not depend on the others and is given by

$$x(t, q, v_{th}) = q + t[v(q) + v_{th}].$$

In any particular stream, v_{th} is constant and therefore does not influence the time of focusing or whether singularities will form. The only effect arises in the coordinates of singularities occurring in different streams. A stream with thermal velocity v_{th} has a singularity at distance $v_{th}t_0$ from the singularity of the "main" stream with $v_{th} = 0$ [here t_0 is the time of singularity formation (2.4)].

Hereafter the velocity dispersion characterized by the dimensionless parameter κ is assumed to be small,

$$\kappa = \frac{\sigma_{th} t_0}{l_0} \ll 1,$$

where

$$\sigma_{th}^2 = \frac{1}{\rho_0} \int v_{th}^2 f_0(v_{th}) dv_{th}.$$

At the time $t_0 = -1/\alpha_0$ [Eq. (2.4)] the density of every stream is given by Eq. (2.7),

$$d\rho(x, v_{th}) = \frac{\rho_0}{3} f_0(v_{th}) dv_{th} \left| \frac{x - v_{th}/\alpha_0}{l_0} \right|^{-2/3} \quad (2.14)$$

Thus the full density can be found by integrating (2.14) over v_{th} . Assuming that $f_0(v_{th})$ is a smooth function with a maximum at $v_{th} = 0$, one easily finds the maximum density at the singular point of the "main" stream ($v_{th} = 0$),

$$\rho_{\max} = \frac{\rho_0}{3} \kappa^{-2/3} \left\langle \left(\frac{v_{\text{th}}}{\sigma_{\text{th}}} \right)^{-2/3} \right\rangle,$$

where

$$\left\langle \left(\frac{v_{\text{th}}}{\sigma_{\text{th}}} \right)^{-2/3} \right\rangle = \frac{1}{\rho_0} \int_{-\infty}^{\infty} \left(\frac{v_{\text{th}}}{\sigma_{\text{th}}} \right)^{-2/3} f_0(v_{\text{th}}) dv_{\text{th}}.$$

A similar estimate of the maximum density at the boundary of a pancake gives

$$\rho_{\max} \approx 2\rho_0 \kappa^{-1/2} \left\langle \left(\frac{v_{\text{th}}}{\sigma_{\text{th}}} \right)^{-1/2} \right\rangle.$$

3. Gas

Now let us consider the motion of an initially cold gas. As before, in the initial state the gas density is assumed to be constant and initial velocity is assumed smooth. The temperature and pressure are taken to vanish.

The motion of cold gas is like the motion of a cold collisionless medium until the first singularities arise. This stage is described by Eqs. (2.1)–(2.3). However, streams of gas cannot penetrate through one another. Gas layers will run into their neighbors, which results in the formation of shock waves, since in a cold gas the speed of sound is equal to zero and therefore the velocity of the gas is supersonic in unshocked gas.

Just after the formation of the first singularities [Eq. (2.7)] at $t_0 = -1/\alpha_0$, two shock-wave fronts arise moving in opposite directions relative to the shocked gas. Simple calculations show that in an ideal gas with adiabatic index $\gamma = C_p/C_v$ the shock fronts move as

$$x_{\text{sh}} = \pm \frac{\gamma-1}{3} \left(\frac{\gamma+2}{3} \right)^{1/2} l_0 \left(\frac{\Delta t}{t_0} \right)^{3/2}, \quad (2.15)$$

where l_0 and t_0 are parameters defined earlier in Eqs. (2.4) and (2.6). It turns out that the pressure of the shocked gas at small Δt remains approximately constant (Fig. 6),

$$p_{\text{sh}} = \frac{\gamma+2}{6} \rho_0 \frac{l_0^2}{t_0^2}. \quad (2.16)$$

The distributions of density and temperature of the shocked gas are

$$\begin{aligned} \rho &= \frac{\rho_0}{3} \left(\frac{\gamma+1}{\gamma-1} \right) \left(\frac{x}{l_0} \right)^{-2/3}, \\ T &= \frac{\mu}{R} \frac{\gamma+2}{2} \left(\frac{\gamma-1}{\gamma+2} \right)^{1/3} \left(\frac{l_0}{t_0} \right)^2 \left(\frac{x}{l_0} \right)^{2/3}, \end{aligned} \quad (2.17)$$

where μ is the molecular mass of the gas, and R is the universal gas constant.

It is interesting to compare the thickness of the shocked gas $2x_{\text{sh}}$ in Eq. (2.15) with the thickness $2x_s$ of the three-stream flow region formed in the case of a col-

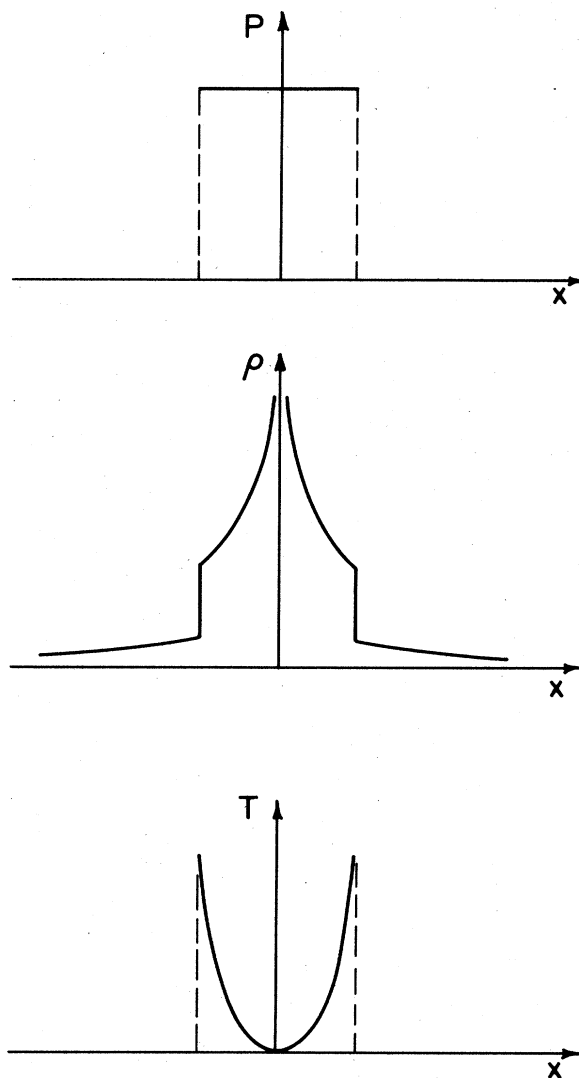


FIG. 6. Distributions of pressure (p), density (ρ), and temperature (T) a short time after the formation of a gas pancake.

lisionless medium according to Eq. (2.8). Assuming the same initial velocity, we find that both quantities depend on same values l_0 and t_0 and therefore their ratio is a constant determined only by γ ,

$$\frac{x_{\text{sh}}}{x_s} = \frac{\gamma-1}{2} (\gamma+2)^{1/2},$$

which equals about 0.64 in the case of $\gamma = \frac{5}{3}$. The mean density of the shocked gas,

$$\bar{\rho}_{\text{sh}} = \frac{3\rho_0}{\gamma-1} \left(\frac{\Delta t}{t} \right)^{-1},$$

is related to that of the collisionless medium inside the three-stream flow region $\bar{\rho}_3$ by Eq. (2.9),

$$\frac{\bar{\rho}_{sh}}{\bar{\rho}_3} = \frac{\rho_{g0}}{\rho_{cm0}} (\gamma - 1)^{-1},$$

where ρ_{g0} and ρ_{cm0} are the initial densities of the gas and the collisionless medium, respectively.

At the shock front, the density jumps by a factor of $(\gamma + 1)/(\gamma - 1)$, and from Eqs. (2.16) and (2.17) the pressure and temperature both fall to zero: the velocity of the gas before entering the shock wave is

$$v = -\frac{q_{sh}}{t} = \pm \left[\frac{\gamma + 2}{3} \right]^{1/2} \frac{l_0}{t_0} \left[\frac{\Delta t}{t_0} \right]^{1/2}.$$

4. Sticky dust

Finally we consider the case of sticky dust. This is the natural limit of a gas system if $\gamma \rightarrow 1$, i.e., of an isothermal gas at $T = 0$.

After formation of the first singularity of the kind (2.7) at the origin, a δ -function singularity develops (Fig. 7). The density behaves like

$$\rho = 2\rho_0 l_0 \left[\frac{\Delta t}{t_0} \right]^{1/2} \delta(x),$$

with its total mass increasing as $(\Delta t/t_0)^{1/2}$. Thus the growth of the masses of the three-stream flow regions in the cases of a collisionless medium, of shocked gas, and of sticky dust is the same:

$$\Delta m \propto (\Delta t/t_0)^{1/2}.$$

B. Late nonlinear stage

From the discussion above, we learned that, starting from similar initial conditions, the motion of the three kinds of medium in question (collisionless medium, gas, sticky dust) develops nonlinear structures of different types: caustics, shock waves, or films of infinite density. In considering the structure of nonlinear things, we used for simplicity a coordinate system moving at the speed of

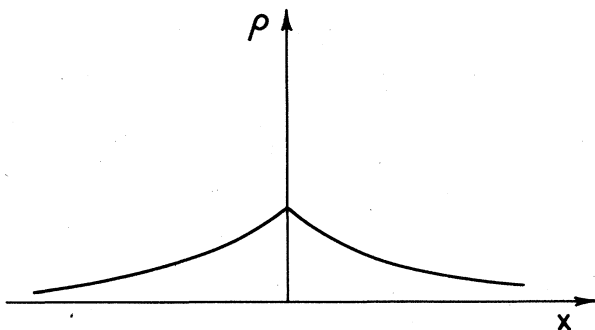


FIG. 7. Density distribution after the formation of a pancake in sticky dust. At the origin there is a δ -type singularity.

clumps of singularities at the moment in question. Mathematically this came from using the local velocity field in the form of Eqs. (2.6) and (2.11). The absence of the term proportional to q^0 does not change the internal structure of nonlinear clumps of matter but brings them to rest. For generic initial conditions [e.g., given by Eq. (2.5)] the nonlinear clumps of matter are never at rest but have finite velocities. This results in collisions and the merging of clumps.

In this section we consider the asymptotic approach of the process toward its final state and examine the statistical properties of density distributions at the late state. Some of these properties depend on the statistics of the initial state. In order to describe a random initial state, we assume that it is specified by a particular—but extremely important—class of Gaussian random fields. The distribution function of such a field is Gaussian and its spatial statistical properties are uniquely specified by a spectrum δ_k^2 that is the ensemble mean square of the Fourier transform of the random function in question,

$$\delta_k^2 \equiv \langle |\delta_k|^2 \rangle$$

and

$$\delta_k \propto \int f(x) e^{ikx} dx. \tag{2.18}$$

Sometimes other characteristics of the Gaussian random field are used, like an autocorrelation function or a structural function, but all of them are uniquely related to the spectrum.

1. Collisionless medium

Here we consider one-dimensional random initial velocity fields $v(q) = d\Phi/dq$ such that the velocity potential $\Phi(q)$ is a Gaussian random function specified by the structural function

$$K(q) \equiv \langle [\Phi(q_1) - \Phi(q_1 + q)]^2 \rangle. \tag{2.19}$$

It is assumed that at small q $K(q)$ has the form

$$K(q) = \frac{D}{2} q^2 - \frac{B}{8} q^4 + \dots$$

In this case one can calculate the distribution function $G(\rho, t)$ of the density at the nonlinear stage as a function of t (Saichev, 1976). Its asymptotic behavior is of particular interest:

$$G(\rho, t) \approx \frac{2}{\sqrt{3} B t^2} \left[\frac{\rho_0}{\rho} \right]^3 \exp \left[-\frac{1}{3 B t^2} \right]. \tag{2.20}$$

The slow decrease of $G(\rho, t)$ at $\rho \rightarrow \infty$ (as ρ^{-3}) is related to the existence of singularities of the kind $\rho \propto x^{-1/2}$. As we shall see, the mean number of singularities per unit length tends toward saturation at $t \rightarrow \infty$.

Another interesting characteristic of the nonlinear stage is the mean number of streams at one point of Euclerian space:

$$\langle N \rangle = 1 + \left[\frac{1}{2\sqrt{3}} + \frac{2Bt^2}{\sqrt{3}} \right] \exp \left[-\frac{23}{24} \frac{1}{Bt^2} \right]. \quad (2.21)$$

At first glance it seems peculiar that $\langle N \rangle$ is greater than 1, even at infinitely small t .

The explanation of this is that the Gaussian character of the potential $\Phi(q)$, as well as its derivatives, results in the existence (with, however, exponentially small probability) of points with a very large velocity derivative $dv/dq = d^2\Phi/dq^2$.

It should be mentioned that at rather small t , whenever $\langle N \rangle \leq 2$, one can estimate, using Eq. (2.21), the fraction of Eulerian space with three-stream flows. In this case one can neglect the region of five or more stream flows and write

$$\langle N \rangle \approx p_1 + 3p_3, \quad p_1 + p_3 \approx 1,$$

where p_1 and p_3 are the probabilities that at a point taken by chance there are one or three flows, respectively. Therefore

$$p_3 = \frac{1}{2}(\langle N \rangle - 1).$$

In the case under consideration, the mean number of singularities per unit length is given by

$$c(t) = \frac{\sigma_1}{\sigma_\alpha} \frac{4}{\pi} \exp \left[-\frac{1}{8\sigma_\alpha^2 t} \right].$$

Here $\sigma_\alpha^2 = \langle \alpha^2 \rangle$ and $\sigma_1^2 = \langle (d\alpha/dq)^2 \rangle$. At $t \rightarrow \infty$ the number of singularities tends to the number of zeros of $\alpha(q) = dv/dq$, which can easily be seen from Eq. (2.2).

These results show that at $Bt^2 \approx 1.5$, the total fraction of Eulerian space with three-stream flows becomes equal to about 50%. At $t \rightarrow \infty$ the mean number of flows at every point increases as $\langle N \rangle \propto Bt^2$, which results in a Maxwellian velocity distribution. However the density fluctuations are non-Gaussian unless coarse graining is applied, because the singularities never disappear.

2. Gas

In analogy with the collisionless case discussed above, gas pancakes form, moving as if the initial velocity field were of a generic type. Due to their motion the gas pancakes occasionally experience collisions that result in the merging of regions of shocked gas and perhaps the formation of new shock-wave fronts.

The intermediate state seems not to be very simple. Chaotic shock waves with progressively decreasing amplitudes gradually transform into random sound waves (acoustic turbulence), propagating in a gas of constant mean pressure but possibly of inhomogeneous mean density and temperature. However, if one takes into account even a small viscosity and thermoconductivity, one easily finds the final state: a gas at rest, whose density is constant and equal to that of the initial state and whose temperature can be easily calculated from the energy conservation law. Probably it is worth mentioning that the

smoothing time for the pressure can be quite different from that of density and temperature.

3. Sticky dust

As we have just seen, density inhomogeneities in either a collisionless medium or a gas decrease as $t \rightarrow \infty$. The evolution of cold sticky matter is quite different, and as we shall see it is at least qualitatively like the evolution of self-gravitating matter in an expanding universe. The density distribution of matter becomes less homogeneous in the course of time. The portion of matter merged into δ -function-like clumps gradually increases, as well as the mean mass of these clumps.

The evolution of density inhomogeneities in matter can be followed in detail because they are described by the well-known Burgers equation (Burgers, 1948, 1974),

$$\frac{\partial v}{\partial t} + v \frac{\partial v}{\partial x} = \nu \nabla^2 v \quad (2.22)$$

supplemented by the equation of continuity

$$\frac{\partial \rho}{\partial t} + \frac{\partial}{\partial x}(\rho v) = 0$$

and the assumption of a homogeneous density distribution at the initial time $\rho(x, t=0) = \rho_0 = \text{const}$ (Gurbatov and Saichev, 1981).

The Burgers equation contains an arbitrary parameter that can be interpreted as the coefficient of viscosity. However the manner in which ν comes into Eq. (2.22) implies the model description of viscosity rather than a physical one. This is the reason why we entitle this section "Sticky dust" instead of "Viscous matter." Cold, sticking matter is described in the limit $\nu \rightarrow 0$, and we shall concentrate our attention on this case. The term on the right-hand side with any nonvanishing value of ν , no matter how small, prevents penetration of one stream of matter through another.

Again it is convenient to use the velocity potential

$$v(x, t) = \frac{\partial \Phi(x, t)}{\partial x}$$

with

$$\Phi(x, t=0) = \Phi_0(x).$$

Making the Hopf-Cole substitution

$$v(x, t) = -\frac{2\nu}{U} \frac{\partial U}{\partial x},$$

we can reduce the Burgers equation to a linear equation of diffusion with respect to U : $\partial U / \partial t = \nu \nabla^2 U$. Its solution, transformed back to the velocity, is

$$v(x, t) = \frac{\int_{-\infty}^{\infty} \frac{x-q}{t} \exp \left[-\frac{G(x, q, t)}{2\nu} \right] dq}{\int_{-\infty}^{\infty} \exp \left[-\frac{G(x, q, t)}{2\nu} \right] dq}, \quad (2.23)$$

where

$$G(x, q, t) = \Phi_0(q) + \frac{(x - q)^2}{2t}.$$

In the case of infinitely small ν describing cold, sticky matter the largest input into integrals (2.23) comes from the vicinity of the smallest minimum of $G(x, q, t)$. In this case one can transform Eq. (2.23) into the much simpler approximate form

$$v(x, t) = \frac{x - q(x, t)}{t},$$

or into the physically more transparent form

$$x = q + tv_0(q), \tag{2.24}$$

which clearly coincides with Eq. (2.1). At small t , derivatives of v are small and the right-hand term in Eq. (2.22) has practically no effect. Therefore its solution in the form (2.24) cannot be doubted, as every particle moves by inertia. Later the situation becomes more complicated. Formal use of Eq. (2.24) apparently predicts overshooting, i.e., in some regions one point x corresponds to three (or even more) points with different q (q_1, q_2, q_3, \dots). Actually, only one of them (say with $q = q_1$) can be at this point. Two others with $q = q_2$ and $q = q_3$ run into a δ -function concentration of matter at a previous stage. At all points q_1, q_2 , and q_3 , $G(x, q_1, t)$ has minima, but at q_1 the minimum is the smallest: $G(x, q_1, t) < G(x, q_2, t)$ and $G(x, q_1, t) < G(x, q_3, t)$.

After merging into a δ -function-type singularity (at $\nu \rightarrow 0$), two other points with $q = q_2$ and $q = q_3$ move differently than is prescribed by Eq. (2.24). The motion of δ -function density peaks is determined by the momentum conservation law. These peaks moving with different velocities merge with each other, swallowing the matter in between and thus growing more massive.

With increasing time, minima of $G(x, q, t)$ approach minima of the initial velocity potential $\Phi_0(q)$. Thus the minima of $\Phi_0(q)$ eventually determine the positions of density peaks in Eulerian space.

More precisely, the coordinates X_{ij} of density peaks can be found from the equation

$$G(X_{ij}, q_i, t) = G(X_{ij}, q_j, t), \tag{2.25}$$

where q_i and q_j are the coordinates of two minima of $G(x, q, t)$. As mentioned above, at large t they are close to the minima of $\Phi_0(q)$. When two peaks merge, the deeper of the two minima survives (the principle of least action works), and the other one does not influence the motion of density peaks afterwards.

At large t , the Eulerian coordinates of density peaks X_{ij} and their velocity V_{ij} are given approximately by the following equations:

$$\begin{aligned} X_{ij} &= \frac{q_i + q_j}{2} + V_{ij}t, \\ V_{ij} &= \frac{\Phi_0(q_j) - \Phi_0(q_i)}{q_j - q_i}, \end{aligned} \tag{2.26}$$

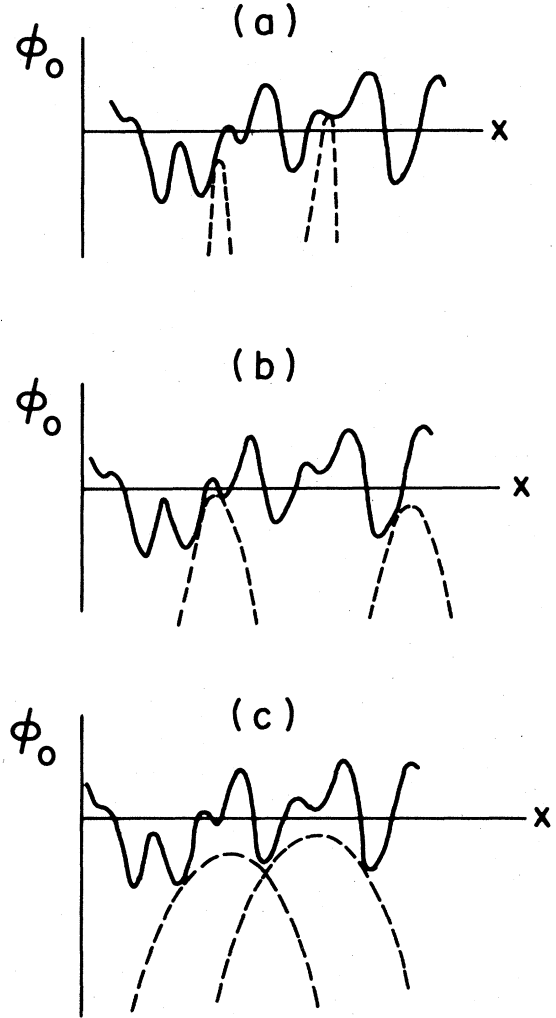


FIG. 8. Three drawings illustrating the geometrical technique for finding the positions of particles and clumps of mass in the sticking dust model at different times. This method is based on the procedure of constructing parabolas tangential to the initial velocity potential provided that crossings are not allowed. The coordinate of the contact point indicates the Lagrangian coordinate of the chosen particles, while the apex of the parabola shows the Eulerian coordinate of the particle. If the parabola has two contact points simultaneously, this means that both particles have come to the same point at this time. All the matter between these particles has been "squeezed" into the same point. The position of the apex shows the position of the clump. (a) At small t parabola $p = -(x - q)^2/2t + H$ (dashed lines) is narrow and it can touch potential $\Phi_0(q)$ (solid line) without crossing it. The top of the parabola shows the current position x of the particle with Lagrangian coordinate q (the coordinate of the contact point). (b) Later the parabola becomes wider and can touch $\Phi_0(q)$ at two points simultaneously: q_1 and q_2 . This means that all particles in between ($q_1 \leq q \leq q_2$) have stuck together in the top point x . Parabolas touching Φ_0 at only one point show the positions of points which have not yet stuck. (c) At large t the parabola becomes so wide that it can touch Φ_0 only in the vicinities of the deepest minima.

where q_i and q_j are the Lagrangian coordinates of two minima determining the position of the peak. There is an interesting geometrical technique for visualizing the search for the minima in question (Fig. 8).

Let us consider the function $\Phi_0(q)$ and imagine a parabola

$$p(x, q, t) = -\frac{(x-q)^2}{2t} + H \quad (2.27)$$

which at a given t and x is gradually elevated by changing H from $H = -\infty$ to some value H_0 where the parabola p touches the curve $\Phi_0(q)$. At large t , p is very shallow and therefore touches $\Phi_0(q)$ at points lying close to the minima of $\Phi_0(q)$. Actually these minima are the deepest ones. Coordinates in the above equation are the positions of the peaks of p , where p touches $\Phi_0(q)$ in two points q_i and q_j simultaneously. The mass of the peak is equal to $\rho_0(q_j - q_i)$, and the momentum equals

$$\rho_0 \int_{q_i}^{q_j} v_0(q) dq = \rho_0 [\Phi_0(q_j) - \Phi_0(q_i)] \quad (2.28)$$

Thus the above equation for the velocity of the peak is just the expression for the momentum-conservation law. This geometrical technique is a vivid method of searching for minima of $G(x, q, t)$, and it is also applicable at earlier stages. It is presented in more detail in the book by Burgers (1974) and the paper by Gurbatov and Saichev (1981).

Finally we note that the motion of sticking matter results in the formation of δ -function-type peaks of density accumulating most of the mass. They move gradually and merge into more massive peaks. At large t , this process is governed by the spatial distribution and by the statistics of the deepest minima of the initial velocity field potential $\Phi_0(q)$.

III. TWO- AND THREE-DIMENSIONAL MOTION OF NONGRAVITATIONAL MATTER

The principal new features of two- and three-dimensional motions are connected with the geometry of the density distribution. At the linear stage the density distribution can be called "structureless." A good example of what we mean by that is a smooth scalar Gaussian field. Later, however, at the nonlinear stage, structures with nontrivial geometry arise. Again we begin with the case of a collisionless, continuous medium.

A. Collisionless medium

The motion of every particle is described by Eq. (1.1). However, in contrast to the one-dimensional (1D) case, the 2D and 3D cases require us to distinguish between different types of initial velocity field:

$$\begin{array}{ll} \text{potential} & \mathbf{v}(q) = \text{grad}\Phi(q), \\ \text{vortex} & \mathbf{v}(q) = \text{curl}\Psi(q), \\ \text{mixed} & \mathbf{v}(q) = A \text{grad}\Phi(q) + B \text{curl}\Psi(q), \end{array}$$

where A and B are constants.

Keeping in mind applications to the gravitational instability process, we shall discuss mainly the potential case.

Using the mass-conservation law, one can obtain an explicit expression for the density as a function of the Lagrangian coordinates and time,

$$\rho(t, \mathbf{q}) = \frac{\rho_0}{\left| \delta_{ik} + t \frac{\partial v_i}{\partial q_k} \right|}, \quad (3.1)$$

where ρ_0 is the initial density, assumed to be constant; $\delta_{ik} = 1$ if $i = k$ and $\delta_{ik} = 0$ otherwise. As $\mathbf{v}(\mathbf{q})$ is a potential vector field, Eq. (3.1) can be written in terms of the eigenvalues $-\alpha(\mathbf{q})$, $-\beta(\mathbf{q})$, and $-\gamma(\mathbf{q})$ of the symmetric tensor

$$d_{ik} = \frac{\partial v_i}{\partial q_k} \equiv \frac{\partial^2 \Phi}{\partial q_i \partial q_k} \quad (3.2)$$

(the negatives are used for historical reasons). We assume that they are ordered in every point of Lagrangian space,

$$\alpha(\mathbf{q}) \geq \beta(\mathbf{q}) \quad \text{and} \quad \beta(\mathbf{q}) \geq \gamma(\mathbf{q}).$$

Equation (3.1) then becomes

$$\rho(t, \mathbf{q}) = \frac{\rho_0}{[1 - t\alpha(\mathbf{q})][1 - t\beta(\mathbf{q})][1 - t\gamma(\mathbf{q})]} \quad (3.3)$$

The eigenvalues α , β , and γ govern the local contraction (or expansion) of matter along three orthogonal directions corresponding to the eigenvectors. To visualize this one can imagine the deformation of the small sphere placed into the point in question. By the time t , the sphere becomes an ellipsoid with axes $r_0(1 - t\alpha)$, $r_0(1 - t\beta)$, and $r_0(1 - t\gamma)$, respectively (here r_0 is the initial radius of the sphere).

At the linear stage, when $|t\alpha| \ll 1$, $|t\beta| \ll 1$, and $|t\gamma| \ll 1$, Eq. (3.3) can be simplified to

$$\rho(t, \mathbf{q}) \approx \rho_0 [1 + t(\alpha + \beta + \gamma)]. \quad (3.4)$$

Thus, at the linear stage, the spatial structure of the density distribution is given by the trace of the deformation tensor,

$$d_{ii} = -(\alpha + \beta + \gamma).$$

Locally the first singularity $\rho = \infty$ arises at the positive maximum α_m of the function $\alpha(\mathbf{q})$ at the time $t = 1/\alpha_m$. It is worth mentioning that in the generic case α is never equal to β or γ at the maxima. Therefore the first singularities originate from a locally one-dimensional contraction of matter.

At the time $t_m = 1/\alpha_m$ the density becomes singular at a single point $\mathbf{q} = \mathbf{q}_m$ where $\alpha = \max$. After a short time Δt has elapsed, the density at this point again becomes finite, but it becomes infinite at the surrounding surface $\alpha(\mathbf{q}) = 1/(t_m + \Delta t) < \alpha_m$. In Lagrangian space the level

surfaces of α in the vicinities of maxima are ellipsoids with three different but comparable axes. In Eulerian space, surfaces of infinite density (caustics) have a quite different shape (Fig. 8). This occurs partly because the motion [Eq. (1.1)] conserves continuity but has one axis much smaller than the two others. The inner structure of the region surrounded by the caustic is similar to that between two singular points in the 1D case discussed before. In cosmology these regions of three-stream flow in 3D are known as "pancakes" (Zeldovich, 1970). Their similarity to 1D "pancakes" (i.e., three-stream flow regions), on the one hand, and 2D or 3D pancakes, on the other, is not only qualitative; the density profiles near singular points obey the same power laws. At the moment of origin of a pancake $t = 1/\alpha_m$ the mean density in a small sphere of radius r centered on the singular point is $\rho(r) \propto r^{-2/3}$ [see Eq. (2.7)], and near most of singular points on the pancake surface $\rho(r) \propto r^{-1/2}$ [see Eq. (2.10) or (2.12)]. However, the pancake surface is not smooth but itself has a singular curve (Fig. 9). In the vicinity of this curve, the density increases as $\rho \propto r^{-2/3}$.

In the course of time the pancake grows both in size and in mass. The thickness of the pancake increases with time as $d \propto (\Delta t/t_m)^{3/2}$, as in the 1D case [Eq. (2.8)], and its diameter grows as $D \propto (\Delta t/t_m)^{1/2}$. Thus, just after formation, the pancake is infinitely thin: $d/D \propto (\Delta t/t_m)$ at $\Delta t \rightarrow 0$. This is connected with the fact that, being a phase velocity, the growth rate of the diameter $dD/dt \propto \Delta t^{-1/2}$ is infinite at $\Delta t \rightarrow 0$. This velocity is not related to the velocity of the fluid relative to the pancake center along the same direction. The latter depends primarily on the other eigenvalues β and γ and therefore can be either positive or negative. This short description summarizes the main properties of pancakes arising as a result of generic potential flow.

B. Similarity with geometric optics

It is quite easy to demonstrate that the 2D motion of collisionless media is similar to the propagation of light in geometric optics (see, for example, Zeldovich, Mamaev, and Shandarin, 1983).

Let us consider a horizontal, transparent plate illuminated from below by columnated light (Fig. 10). The plate has a flat base at the plane $r=0$ and a smoothly

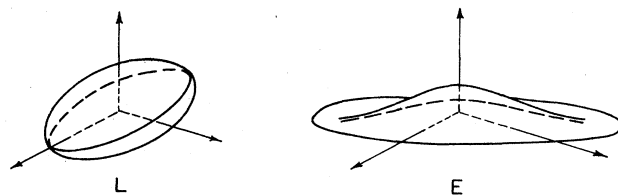


FIG. 9. A surface $\alpha = \text{const}$ in the vicinity of $\alpha = \text{max}$, both in L (Lagrangian) and E (Eulerian) spaces at time $t = 1/\alpha$. At this time the surface $\alpha = \text{const}$ is a caustic in E .

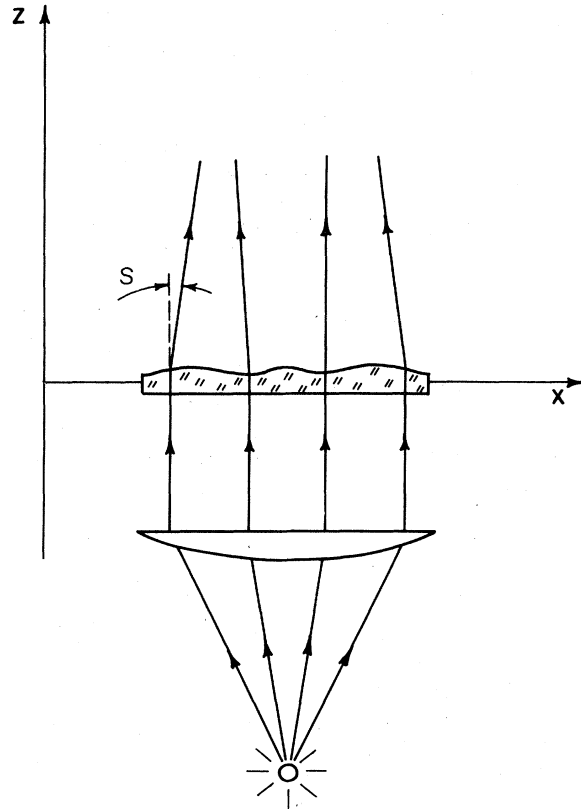


FIG. 10. The scheme of an optical experiment simulating the formation of the cellular structure in 2D.

varying thickness specified by a function $h = h(x, y)$. When the rays pass through such a plate they are deflected somewhat differently at different points. We denote the deflection angle by s , which determines the direction of the ray after passing through the plate. All deflection angles are assumed to be small and the plate to be thin. The two-dimensional coordinates of the ray entering the plate at the point with coordinates $\mathbf{q} = (q_1, q_2)$ depend on z and are

$$\mathbf{r}(z, \mathbf{q}) = \mathbf{q} + z\mathbf{s}(\mathbf{q}), \tag{3.5}$$

where

$$s_i(\mathbf{q}) = -(n - 1) \frac{\partial h(\mathbf{q})}{\partial q_i} \tag{3.6}$$

(n is the refractive index of the plate, which for simplicity is assumed to be independent of the wavelength of light). Putting the screen at some distance z from the plate, one will see an inhomogeneous distribution of brightness. Denoting the brightness by the same letter as the density of fluid in the mechanical case, one obtains

$$\rho(z, \mathbf{q}) = \frac{\rho_0}{[1 - z\alpha(\mathbf{q})][1 - z\beta(\mathbf{q})]}, \tag{3.7}$$

where $\alpha(\mathbf{q})$ and $\beta(\mathbf{q})$ are the principal curvatures of the surface $h = h(\mathbf{q})$. Of course, they are equal to the eigen-

values of the tensor $\partial^2 h / \partial q_i \partial q_k$.

Comparing Eqs. (3.5) and (3.7) with (2.1) and (2.2) or with (1.1) and (3.3), one immediately notes the similarity of the optical example to the mechanical problems discussed before. The plate thickness h is analogous to the velocity potential, and the vertical coordinate z is analogous to the time.

With obvious modifications one can consider the reflection of light from a curved surface instead of the propagation of light through a transparent plate. Perhaps everyone has observed the peculiar pattern of bright spots at the bottom of a shallow pool of water or at a bridge vault emerging on a sunny day when sunlight refracts or reflects at the surface of rippled water (Fig. 11). This pattern resembles a distorted honeycomb structure, in which large dark regions are separated by bright, relatively narrow "walls."

An essential feature of optical systems is the potential form of initial perturbations; the potential is the function defining the refracting or reflecting surface. If the surface is curved along one direction only [$h = h(x)$], then such a system simulates the one-dimensional motion of a collisionless medium.

The structure discussed above is an example of intermediate asymptotics. At $z \rightarrow \infty$ after many intersections of the rays of monochromatic light the distribution of brightness on the screen represents a speckle field, i.e., a nonstationary (at given z), spotty distribution of bright-

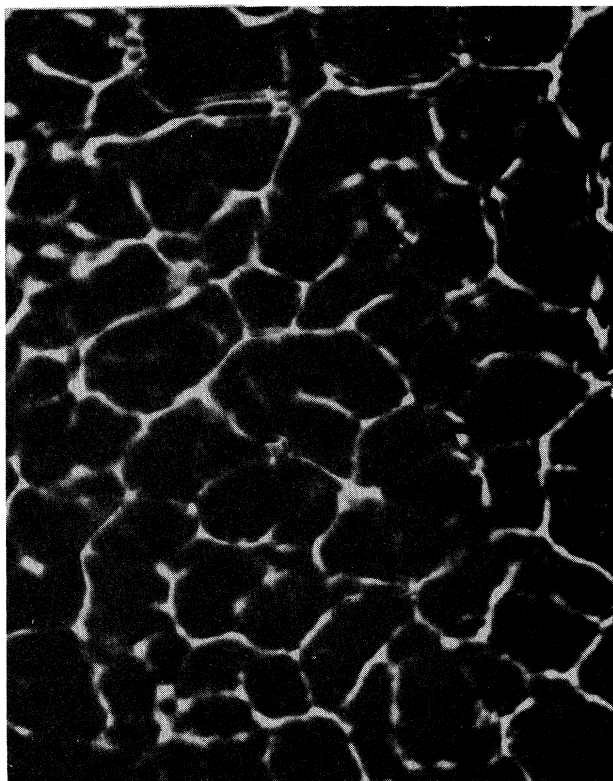


FIG. 11. Distribution of brightness on the screen in the optical experiment shown in Fig. 10.

ness caused by the wave nature of light (see, for example, Baranova *et al.*, 1983).

C. Motion as mapping and catastrophe theory

From the mathematical point of view both the motion of collisionless particles in mechanics and the propagation of rays of light in geometrical optics are a one-parameter (t or z) family of differentiable mapping. After a time t , the mapping assigns a point with coordinates q in Lagrangian space (L) to its final position x in Eulerian space (E).

The case of particular interest is the gradient mapping having the form $q \rightarrow \partial f / \partial q$.

For sufficiently short times t , the mapping is one-to-one. However, as we have already seen, as time passes the particles begin to overtake one another and the mapping develops singularities. Surfaces of infinite density arise in E . This means that infinitely close particles from L arrive at the same point in E .

The very-well-known example of the focusing of light rays at a single point by a spherical lens is not typical from our point of view because it is the result of a very special (not generic) initial field $s(\mathbf{q})$. In generic cases the set of singular points forms a caustic, i.e., a closed surface in 3D or a closed line in 2D. In turn caustics also have singularities like cusps; however, overly complicated singularities are unstable. Infinitesimal, smooth variations of the function defining the mapping cause the decay of unstable singularities into stable ones.

Generic (i.e., stable) caustics in one-, two-, and three-dimensional space have only standard singularities. It is not easy to imagine even the simplest caustics in 3D.

The simplest mathematical models for singularities are called normal forms. They give a local field $\Phi(q)$ [Eq. (1.4)] in the form of elementary polynomials containing a few parameters. The singularities arise at critical values of these parameters.

In 1D motions of collisionless media, there are only two kinds of generic singularities, A_2 and A_3 according to Arnold's classification (Arnold, 1972, 1982, 1986). The former is the boundary of pancakes and can exist at any moment of time. The latter exists only at particular moments when a pancake originates. In 2D and 3D there are a few more kinds of singularities as well as metamorphoses. All of them are known for the gradient mapping. One can find their normal forms in the paper by Arnold (1982) or in the book of Arnold, Gusein-Zade, and Varchenko (1985).

It is interesting that the points of the potential field $\Phi(\mathbf{q})$ giving the mapping (1.1) are specified by conditions with a very simple geometrical meaning (Arnold *et al.*, 1982; Rozhanskij and Shandarin, 1984). To discuss this, one needs to use the following quantities. Differentiating the scalar field $\Phi(q)$ twice, one can find a tensor field $d_{ik}(\mathbf{q}) = -\partial^2 \Phi / \partial q_i \partial q_k$, three fields of its eigenvalues $\lambda_i(\mathbf{q}) = \{\alpha(\mathbf{q}), \beta(\mathbf{q}), \gamma(\mathbf{q})\}$, and eigenvector fields $\mu^{(l)}(\mathbf{q}) = \{\mu^{(\alpha)}(\mathbf{q}); \mu^{(\beta)}(\mathbf{q}); \mu^{(\gamma)}(\mathbf{q})\}$ belonging to these ei-

genvalues. As before, the eigenvalues are supposed to be ordered in every point: $\alpha \geq \beta$ and $\beta \geq \gamma$.

The origin of the pancakes is connected with the metamorphosis specified as $A_3(++)$ and takes place at the positive maxima (as we consider $t > 0$) of the greatest eigenvalue $\alpha(\mathbf{q})$.

The newborn pancake is bounded by a caustic which is the map in E of the level surface $\alpha(\mathbf{q}) = \text{const}$. Almost all points of this surface are singularities of the kind A_2 discussed before. The exceptions are points A_3 forming the edges of the pancake. In L (i.e., Lagrangian space), points A_3 are specified by the condition that the vector $\mu^{(\alpha)}$ and the level surface $\alpha(\mathbf{q}) = \text{const}$ touch. Sets of A_3 points form surfaces. At any moment t , the level surface $\alpha(\mathbf{q}) = 1/t$ cuts out the line on the surface A_3 . The map of this line in E (i.e., Eulerian space) is the edge of a pancake.

There are also points where the vector $\mu^{(\alpha)}$ is tangential to the surface A_3 (i.e., the set of points A_3). They are classified as A_4 and are called "swallowtail" points. In L , the set of such points forms lines. The swallowtail points play an important role, connecting pancakes in the joint cellular structure.

Finally, vector field $\mu^{(\alpha)}(\mathbf{q})$ is tangential to lines A_4 in individual points called A_5 .

Some types of singularities are situated at a set of individual points. They form at individual moments of time and are called metamorphoses of caustics, as they are subsets of caustic surfaces. An example of metamorphoses are the maxima of $\alpha(\mathbf{q})$ [called $A_3(++)$], where pancakes originate. In the saddle points of $\alpha(\mathbf{q})$ [called $A_3(+ -)$] pancakes merge with each other.

Conditional maxima of $\alpha(\mathbf{q})$ lying on lines A_4 [called $A_4(+)$] are points where "swallowtail singularities" originate. In the conditional minima of $\alpha(\mathbf{q})$ lying on A_4 [called $A_4(-)$] two swallowtails conjoin.

It is worth recalling that we consider events only at $t > 0$; thus points of positive α are under consideration.

The regions of positive α in L can contain the region of positive β , which by our definition is not greater than α . There are also regions of positive γ within the positive β region. In all of them there are similar singularities defined by similar conditions involving level surfaces of $\beta(\mathbf{q})$ and $\gamma(\mathbf{q})$ corresponding to fields of eigenvectors $\mu^{(\beta)}$ and $\mu^{(\gamma)}$. These fields give rise to their singularities even later. If the initial potential $\Phi_0(\mathbf{q})$ (1.4) is a smooth Gaussian random field, then the fractions of matter passing through the α , β , and γ caustics (i.e., caustics related to α , β , and γ) are, respectively, about 92%, 50%, and 8%; these numbers are the fractions of the volume where α , β , and γ are positive (Doroshkevich, 1970). In 2D the area with $\alpha > 0$ is about 79%, and with $\beta > 0$ is about 21%. These numbers are given again for Gaussian fields.

We have briefly discussed the singularities connected with only one of three eigenvalues at the given point. However, in 3D there is a set of points forming lines where $\alpha = \beta$ or $\beta = \gamma$ (note that points with $\alpha = \beta = \gamma$ do not exist in generic fields). These lines give rise to singu-

larities specified as D_4 , of which there are two kinds: D_4^+ , also called "purse" or "hyperbolic umbilic" singularities in catastrophe theory, and D_4^- , called "pyramid" or "parabolic umbilic." In addition there are points $D_4(+)$ and $D_4(-)$ on lines D_4 where singularities of corresponding kinds originate and conjoin. Finally there are also points on lines D_5 where metamorphoses of D_4^+ into D_4^- and vice versa take place.

This short enumeration gives the full list of kinds of singularities and metamorphoses arising in generic 3D potential flows. They are examples of perturbation growth in a zero-temperature collisionless medium.

One can find more details in papers by Arnold (1972, 1982, 1986), Arnold *et al.* (1982), and Rozhanskij and Shandarin (1984).

D. Topology of the regions of multistream flows

The first regions of three-stream flows originating as pancakes grow rather quickly in diameter. Some of them change their shapes by means of the swallowtail metamorphosis, and the process of conjunction begins.

Relatively quickly the regions of multistream flow form a joint structure. Probably the most familiar 2D example of such a structure is the bright pattern mentioned above that sometimes occurs at the bottom of a shallow pool of water due to refraction of initially parallel light beams by a rippled surface. Regions where three or more beams of light fall are generally brighter. The boundaries between bright and dark regions are especially bright, since they are caustics.

Our ideas about network structure have come from the impression that the dark regions are generally separated from one another, despite the fact that the total area occupied by them is greater than that of the bright regions. In contrast, the bright regions form a connected cellular structure.

If the plane were divided into bright and dark regions by chance one might naturally expect regions occupying less area to be separated.

Let us discuss this question in detail. It turns out that a good statistics characterizing the topological properties of random fields is percolation statistics (Zeldovich, 1982a, 1983; Shandarin, 1983b; Shandarin and Zeldovich, 1983, 1984).

The natural example to start the discussion is a smooth random Gaussian field. This is a good approximation to the brightness distribution at small distances from the rippled surface of water or for the density distribution at the linear stage. In both cases it is supposed that the refracting (or reflecting) surface or the potential generating the initial velocity field is a Gaussian random function.

Let us divide the space in 3D (or the plane in 2D) into two kinds of regions: "bright" regions where the Gaussian field f is greater than some level f_c and "dark" regions with $f < f_c$. Generally speaking, the structure of regions of both kinds is pretty complicated. There can be large bright "continents" with dark "lakes" and bright

“islands” in the lakes or vice versa. Apparently these structures change with changing f_c .

By definition we shall call regions of one kind “connected” if they percolate. This means that there is an infinite cluster between the clusters in question. (According to percolation theory, every individual region separated from others is called a cluster.) An infinite cluster means a connected region that cannot be contained in a sphere of finite radius.

In the case of 2D Gaussian fields there is percolation along (say) bright regions if the total area occupied by them exceeds about 50%. (However, this has not been strictly proven.) There is a possibility that the percolation threshold is somewhat higher $(50+\epsilon)\%$. In the range from $(50-\epsilon)\%$ to $(50+\epsilon)\%$ neither bright nor dark regions percolate (Menshikov *et al.*, 1986). It should be noted that this does not break symmetry between bright and dark regions, because in this range neither phase percolates.

The question becomes more complicated in 3D. There are three possibilities: (1) the dark phase percolates but the bright one does not, (2) vice versa, and (3) both bright and dark phases percolate. Thus there are two thresholds in the fraction of volume occupied by one of the phases when transitions from (1) to (3) and from (3) to (2) take place. In the case of Gaussian random fields, a phase occupying less than about 16% of the total volume does not percolate; otherwise it does percolate (Skal *et al.*, 1973). It is worth mentioning an interesting coincidence: 16% is also the fraction of the total volume in which the Gaussian field exceeds the 1σ level above the mean value.

These numbers seem to be in general agreement with intuitive ideas about random fields, at least in 2D. But this picture clearly is unlike the nonlinear distributions of brightness (Fig. 11) or density (Fig. 12) having non-Gaussian types, where in contrast to the Gaussian case, bright and dense regions percolate occupying markedly less area than dark or rarified ones.

With Gaussian fields, one can speak of structures associated with two phases of the volume, a “bright” phase in which $f > f_c$ and a “dark” phase in which $f < f_c$. Non-Gaussian fields, however, can also possess structures of some kind, being in a sense independent of the chosen level of f_c . The idea is to use percolation thresholds as statistical parameters characterizing the topological properties of a non-Gaussian random field (Shandarin, 1983b). Starting from a very high level and lowering it, one can find the volume fraction v_1 occupied by bright regions (where $f > f_{c1}$ at the percolation threshold). Keeping in mind the limiting case $v_1 \rightarrow 0$ for a three-dimensional cobweb, we find it natural to specify the random field in question as a network structure if $v_1 < 0.16$. If the other percolation transition that stops percolation along a dark region (where $f < f_{c2}$) takes place at $v_2 < 0.84$, then the random field can be specified as a cellular structure. Again we have an evident limiting case of a honeycomb structure with infinitely thin walls where

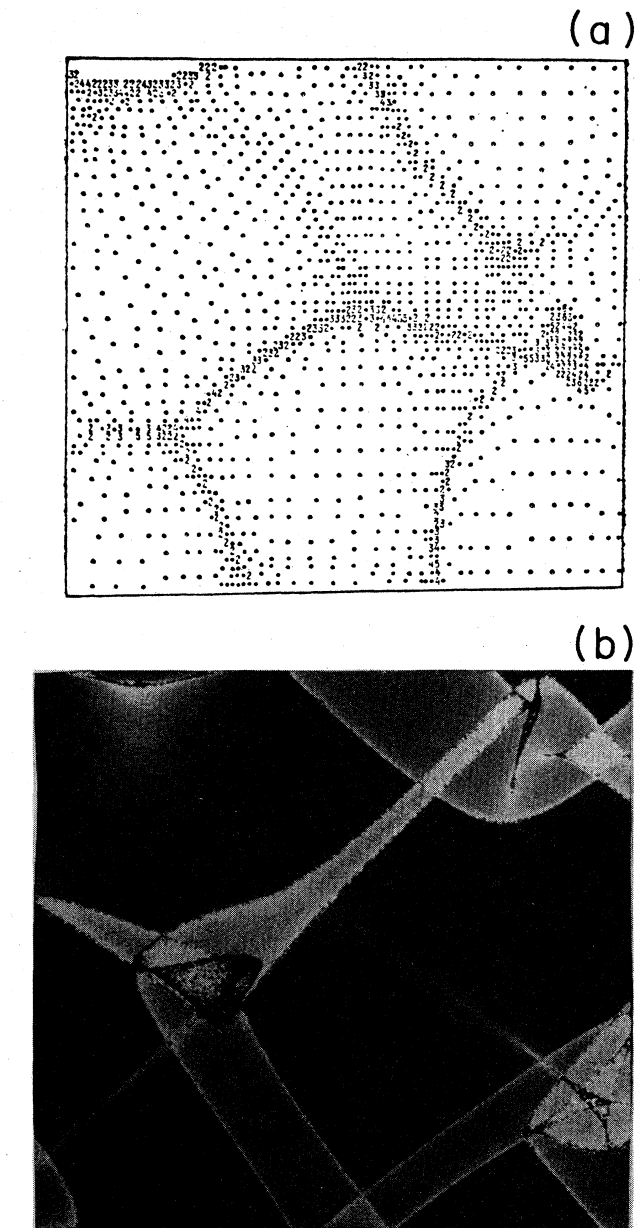


FIG. 12. Distribution of particle density at the early nonlinear stage in 2D: (a) poor resolution (Shandarin, 1975); (b) fine resolution (Buchert, 1988).

$v_2 \rightarrow 0$. If the field is positive ($f > 0$), as with density or brightness distributions there are additional natural parameters at the thresholds. They are the fractions of mass (or light) in bright regions at the percolation thresholds. The larger they are, the more distinct the structure.

Returning to the formation of structure at the nonlinear stage of the evolution of density perturbations, let us recall that the process begins from the origin of three-stream flow regions. Their boundaries in E are mappings of the level surfaces of α in L , which can be directly seen from Eqs. (3.2) and (3.6). In contrast to perturbations

$\delta\rho/\rho$, which are a Gaussian random field where regions of positive ($\delta\rho/\rho > 0$) and negative ($\delta\rho/\rho < 0$) perturbations occupy equal volumes (or areas in 2D), regions of positive α occupy about 79% of the total area in 2D and about 92% of the total volume in 3D (Doroshkevich, 1970). Both numbers are somewhat greater than the percolation thresholds in Gaussian fields (50% in 2D and 84% in 3D); thus it is safe to suppose that regions of positive α percolate in L . In contrast, regions of negative α do not percolate.

What is extremely important is that the mapping (1.1) from L to E is continuous. This means that every two neighboring points in L remain neighbors in E . (The converse, incidentally, is not true.) Therefore the mapping (1.1) conserves the topology. Every closed line in L is transformed into a closed line in E .

As we have learned, during the growth of density inhomogeneities, the regions of positive α generally contract and the regions of negative α expand. Thus the regions of negative α remain isolated and increase their fraction of volume. This is the main qualitative reason for the formation of cellular structure at the beginning of the nonlinear stage (Zeldovich, 1982a).

Assuming that the field of α has about the same percolation thresholds as a Gaussian field, one can find that the fraction of volume necessary for percolation is about 16%, and this threshold in terms of α means that $\alpha > \alpha_{16\%} \approx 2\sigma_d$ [here $\sigma_d^2 = \langle (\partial^2\Phi_0/\partial q_i\partial q_k)^2 \rangle$ is the dispersion of the deformation tensor components (3.2)]. Using this estimate one can calculate the time when these level surfaces become caustics, $t = 1/\alpha_{16\%}$. At this time, the mean density perturbations [predicted by linear equation (3.4)] reach a value of only about $\delta\rho/\rho \equiv \langle (\delta\rho/\bar{\rho})^2 \rangle^{1/2} \sim 1$. This means that percolation along multistream flow regions arises at the very beginning of the nonlinear stage. At this time the fraction of the total volume occupied by them in E is 2–3 times less than 0.16, and this produces the impression of very distinct network structure. Similar estimates are also possible in 2D, where the threshold is $\alpha \approx \alpha_{50\%} \approx 0.75\sigma_d$.

In considering the evolution of density inhomogeneities in a collisionless medium, one must not use these simple arguments for too late times. The reason is that the contraction of a volume element ceases after passing the singularity and begins to expand. Ultimately it results in expansion of the multistream flow regions to the total volume. It is even very doubtful that cellular structure (in the above sense) can be formed by multistream flow regions in a collisionless medium in 3D.

By contrast in sticky matter, cellular structure arises quite easily. This will be discussed later when we consider a self-gravitating medium and cosmology.

IV. GRAVITATING MATTER. COSMOLOGY

Surprisingly, the above consideration of examples of motion in different media (collisionless particles, gas, sticky particles) in the absence of gravitation turns out to

be a very good preparation for the study of nonlinear gravitational instability on the scale of clusters and superclusters of galaxies. For physicists having interests far from astronomy and cosmology, we recall that clusters and superclusters of galaxies, along with the voids between them, are the principal elements of the large-scale structure of the universe. The scales in question are from about 1 Mpc $\approx 3 \times 10^{24}$ cm to a hundred or perhaps a couple of hundred Mpc. On the scale of these giant structures, even dark matter galaxy halos having typical sizes of several tens of kiloparsecs can be considered as point concentrations of mass. On the other hand, large-scale structure is still much less than the horizon scale $ct_0 \sim 10^4$ Mpc; therefore, for the description of motions that result in large-scale structure formation, one can safely use a Newtonian description of mechanics and gravitation (Bonnor, 1957; Peebles, 1980; Zeldovich and Novikov, 1983).

The problem of large-scale structure has at least two aspects. First, to describe and explain the present large-scale structure one needs to develop a nonlinear theory of gravitational instability that becomes important at a recent epoch, say at $z \sim 5$. [Here z is the redshift and is used to indicate the epoch in cosmological evolution; at present $z = 0$, while at the big bang $z \rightarrow \infty$. The overall size of the universe at epoch z is $(1+z)$ times less than now.] Considering the smaller scales of galaxies, one must remember the importance of gas dynamic and thermal processes in the baryon component.

Second, to study density inhomogeneities at the nonlinear stage, one needs to know the primordial distortions of homogeneity of the universe. It is generally accepted that these distortions arise as quantum fluctuations in the inflationary universe (see, for example, Peebles, 1984b; Kofman and Linde, 1987). Later, at the Friedmann stage, the relevant perturbations exist in the form of standing waves having random phases. Although perturbations of gravitational wave types must be present in the universe, they exert no influence upon the formation of large-scale structure. We mention the problem of primordial fluctuation origin only because its solution is unavoidable in the full theory of structure formation.

A. Dark matter in the universe

Astronomers encountered the problem of dark matter about half a century ago while studying the dynamics of rich clusters of galaxies (Zwicky, 1933). Recent investigations have shown that luminous matter of all kinds, including stars, gas, and dust, comprises only a small fraction of the total mass of the universe (see, for example, recent reviews by Einasto *et al.*, 1987, and Trimble, 1987). Basic arguments for the existence of dark matter come from data about the rotation of spiral galaxies and, as we have already mentioned, about the motions of galaxies in clusters of galaxies. Fast rotation of hydrogen clouds far outside the luminous discs of spirals, as well as high-velocity dispersion of galaxies in clusters, indicates

deep gravitational potential wells. Neither in individual galaxies nor in clusters can the strength of the gravitational field be explained by the luminous matter.

The theory of nucleosynthesis in the framework of big bang cosmology puts severe limits on the mean density of baryons. The theoretical predictions of the abundances of light elements H, D, ^3He , ^4He , and ^7Li can be reconciled with observations only in a low-baryon-density universe, $\Omega_b h_{50}^2 \leq 0.14$ (Olive *et al.*, 1981), where $\Omega_b = \bar{\rho}_b / \rho_{\text{cr}}$, $\rho_{\text{cr}} = 3H_0^2 / 8\pi G \approx 5 \times 10^{-30} h_{50}^2 \text{ g cm}^{-3}$, and $h_{50} = H_0 / (50 \text{ km s}^{-1} \text{ Mpc}^{-1})$. The dimensionless parameter Ω characterizes the overall geometry of the Friedmann universe and its future fate. If the total value $\Omega_t > 1$, the universe is closed and eventually will cease to expand and finally collapse. The cosmological model with the critical value of the total mean density $\Omega_t = 1$ ($\bar{\rho}_t = \rho_{\text{cr}}$) is the flat Friedmann-Robertson-Walker universe, which will expand forever; observations restrict $1 \lesssim h_{50} \lesssim 2$, and thus $\Omega_b \leq 0.14$.

However, if most of the mass of the universe is in baryons, one encounters serious difficulty in explaining the observed structure formation. The observational upper limits on anisotropies of the microwave background radiation, $\Delta T / T \lesssim 3 \times 10^{-5}$ over the range of angular scales from minutes to quadrupole (see, for example, Melchiorri *et al.*, 1986), impose very strong restrictions on the type, spectrum, and amplitude of density fluctuations at the decoupling epoch (Sec. IV.F). These restrictions are especially severe in open universes (Guyot and Zeldovich, 1970). In addition, the theoretically very attractive and popular model of the inflationary universe predicts a flat universe $\Omega_t = 1$. The cosmological constant Λ can also contribute to Ω_t if $\Lambda \neq 0$. However the Λ term does not help to solve the problem in question, since it was devised to describe a model with homogeneous density $\rho_\Lambda = c^2 \Lambda / 8\pi G$.

Thus, on the basis of the arguments mentioned above, astrophysicists have come to the conclusion that the most probable candidates for constituents of dark matter are weakly interacting massive (i.e., $m \neq 0$) particles (Marx and Szalay, 1972; Cowsik and McClelland, 1973; Szalay and Marx, 1976). At present they dominate the mean density of the universe, possibly amounting to as much as $\Omega_{\text{DM}} \sim 0.9 - 0.99$. They interact solely due to gravitation and thus can influence the dynamics of galaxies or more massive objects.

Current theories of elementary particles suggest a lengthy list of weakly interacting particles as possible candidates for dark matter. There are neutrinos of electronic or other kind (if they possess masses about 10–100 eV), photinos (supersymmetric partners of photons), axions (pseudoscalar bosons suggested by theorists to avoid strong violation of CP symmetry in strong interactions), and others in the list (for reviews, see Primack, 1986, and Turner, 1987).

The microwave background radiation, with a temperature $T_\gamma \approx 2.7 \text{ K}$, gives $\Omega_\gamma \approx 10^{-4}$. If neutrinos are massless (and cannot cluster), they also contribute about

$\Omega_\nu \sim 10^{-4}$ and therefore are unimportant as candidate constituents for dark matter in this case.

At late stages when nonlinear effects become important, weakly interacting particles behave like collisionless dust. The baryon component, which plays a crucial role in the formation of galaxies and stars, is a perfect gas at pregalactic stages. Thus all examples discussed above are related to some extent to the problem of large-scale structure formation. As we shall see, gravitational attraction sometimes can be approximately described by sticking of particles.

B. Linear gravitational instability

Large-scale density inhomogeneities grow with time under the action of gravity (Lifshitz, 1946; Lifshitz and Khalatnikov, 1963). The microwave background radiation data on angular anisotropies show that, at the epoch of the last scattering at $z_d \simeq 1400$, when radiation decoupled from matter, the density distribution of the universe was almost homogeneous, $\delta\rho/\rho < 1$, and its evolution is perfectly described by the linear theory given in textbooks on cosmology (see, for example Peebles, 1980; Zeldovich and Novikov, 1983). Here we briefly mention only some results of linear analysis relevant to our topic.

Evolution of density fluctuations depends both on epoch and on scale. This results in changing of the spectrum of density fluctuations. In turn the shape of the spectrum at the dustlike stage determines the essential features of nonlinear processes resulting in the origin of galaxies and large-scale structure.

In accord with a widely accepted idea, we assume that the primeval perturbations originated at the inflationary stage (Starobinsky, 1980; Guth, 1981; Linde, 1982, 1984). They seem to have been generated as null quantum fluctuations (i.e., irreducible at $T=0$) of a scalar field or metric. The idea of null quantum fluctuations was first suggested by Sakharov (1965), in the framework of the presently unacceptable model of a cold universe (not to be confused with the cold dark matter universe). The most attractive idea seems to be that of simple adiabatic density perturbations (Harrison, 1970; Zeldovich, 1972). In this case the long-wave part of the density perturbation spectrum at the linear stage after, say, decoupling is independent of the kind of weakly interacting particles that constitutes the dark matter and obeys a simple power law,

$$\delta_k^2 \propto k \quad \text{at } k \lesssim k_{\text{eq}}. \quad (4.1)$$

Here $k = 2\pi a(t)/\lambda$ is the comoving wave vector, while k_{eq} corresponds to the horizon at the epoch of equality, when the density of radiation is equal to the density of nonrelativistic matter (Sec. IV.D). However, the shape of the spectrum at shorter scales $k > k_{\text{eq}}$ crucially depends on the kind of particle dominating the mean density of universe.

C. Hot and cold dark matter

The most important characteristic of weakly interacting particles during the linear evolution of density perturbations is the value of their thermal velocities. This is because all density perturbations with scales less than the horizon size damp completely at the relativistic stage due to free streaming (Doroshkevich *et al.*, 1981). In contrast, once nonrelativistic they begin to slow down and quickly become a cold-dust-like medium. At this stage surviving density perturbations grow at the rate $\delta\rho/\rho \propto a$ if nonrelativistic particles dominate the mean density; otherwise perturbations, while not completely damped, remain only stagnant (Guyot and Zeldovich, 1970; Meszaros, 1974). To summarize, one can conclude that all perturbations with scales smaller than the horizon damp when weakly interacting particles become nonrelativistic, and the spectrum of perturbations acquires a sharp cutoff at short wavelengths.

The value of the cutoff scale is a very important parameter characterizing the formation of large-scale structure, as it determines the scale of the first nonlinear clumps (i.e., inhomogeneities attaining $\delta\rho/\rho > 1$) and the time sequence of the formation of large-scale objects.

Neutrinos are an example of hot dark matter (HDM), as they become nonrelativistic at a rather late stage,

$$1+z_\nu \approx 6 \times 10^4 \frac{m_\nu}{30 \text{ eV}}, \quad (4.2)$$

where z_ν is the redshift and m_ν is the neutrino mass in eV. At this epoch the horizon scale corresponds to the typical size of large-scale structure and in mass units is about

$$M_\nu \sim 2 \times 10^{15} \left[\frac{m_\nu}{30 \text{ eV}} \right]^{-2} M_\odot, \quad (4.3)$$

where $M_\odot \approx 2 \times 10^{33}$ g is the mass of the Sun. M_ν can be expressed through fundamental constants $M_\nu \approx m_{\text{Pl}}^3 m_\nu^{-2}$ [here $m_{\text{Pl}} = (\hbar c / G)^{1/2}$ is the Planck mass; Bisnovaty-Kogan and Novikov, 1980].

HDM cosmological models lead to the so-called "top-down" scenario for large-scale structure formation. This means that the first objects to form are pancakes of supercluster sizes, and galaxies form later by fragmentation of the pancakes (Sunyaev and Zeldovich, 1972; Doroshkevich and Shandarin, 1974; Shandarin *et al.*, 1983; Silk *et al.*, 1983; Zeldovich, 1984). One particular variant of the HDM model assumes that particles are unstable, with a lifetime $\sim 3 \times 10^9$ yr (Doroshkevich and Khlopov, 1984), resulting in somewhat better agreement of the model with observations.

In cold dark matter (CDM) cosmology, the scale of the cutoff in the spectrum of perturbations is too small to be of any importance for large-scale structure formation. A cutoff of small scale can happen for either of two reasons. First, the mass of particles might be so large that they become nonrelativistic very early. Second, there are particles like the axion that never were in thermal equilibrium

and thus have a very low thermal velocity dispersion despite their small masses.

In CDM models the formation of astronomical objects begins with globular star clusters with a mass of about $10^6 M_\odot$; later, galaxies form, and finally clusters and superclusters. This is the "bottom-up" scenario (Gott and Rees, 1975; Peebles, 1980; Blumenthal *et al.*, 1984; Primack and Blumenthal, 1984).

Warm dark matter (WDM) models have also been suggested, with a cutoff in the density perturbation spectrum in the range of galaxy masses. However, at present WDM models seem to be unpopular, mostly due to the lack of good candidate particles (see, for example, Primack, 1986).

D. Equality epoch

There is another epoch in the history of the universe that is also important from the point of view of the evolution of density perturbations. At this time the density of the nonrelativistic component becomes equal to that of the relativistic component. Earlier the universe is radiation dominated, while later it becomes matter dominated. (Detailed discussions of the question, including other possibilities, can be found in the review of Poinarev and Khlopov, 1985.)

In a radiation-dominated universe, perturbations on a scale larger than the horizon grow as a^2 . In contrast, the growth of perturbations [or nonrelativistic weakly interacting particles with wavelengths shorter than the horizon experience stagnation (Guyot and Zeldovich, 1970; Meszaros, 1974). This effect produces a bend in the spectrum of density fluctuations from the initial power-law index n to $n-4$ at the scale of the horizon at the equality epoch (Peebles, 1980). A detailed consideration has shown that the standard inflationary spectrum (the so-called Harrison-Zeldovich spectrum), having a power-law form in long waves $\delta_k^2 \propto k$ ($k < k_{\text{eq}}$), acquires the form $\delta_k^2 \propto k^{-3} \ln^2 k$ (at $k \gg k_{\text{eq}}$) (Primack and Blumenthal, 1984; Starobinsky and Sahni, 1984).

The transition from radiation to matter domination takes place at

$$(1+z_{\text{eq}}) \approx 10^4 \Omega h_{50}^2 (1+0.68N_\nu), \quad (4.4)$$

where N_ν is the number of massless neutrino species. The mass of particles contained in the horizon size volume is about

$$M_{\text{eq}} \approx 10^{16} (\Omega h_{50}^2)^{-2} M_\odot, \quad (4.5)$$

and the comoving linear scale is

$$R_{\text{eq}} \approx 40 (\Omega h_{50}^2)^{-1} \text{ Mpc}. \quad (4.6)$$

It is interesting to note that M_{eq} is close to M_ν for m_ν , several tens of eV. Thus in a neutrino-dominated universe the spectrum of density fluctuations has practically only one scale.

E. Spectrum of density fluctuations at $z < z_{\text{eq}}$

In this section we present the results of calculations of the density fluctuation spectrum for weakly interacting particles after they have passed the epoch of equality. As a very crude approximation to the spectrum, one can see

$$\delta_k^2 = A \times \begin{cases} \frac{k}{k_{\text{eq}}} & \text{at } k < k_{\text{eq}}, \\ \left[\frac{k}{k_{\text{eq}}} \right]^{-3} & \text{at } k_{\text{eq}} < k < k_v, \\ 0 & \text{at } k_v < k, \end{cases} \quad (4.7)$$

where k_{eq} and k_v are related approximately to M_{eq} and M_v as $M \sim \bar{\rho} k^3$; M_v denotes the mass of matter within the horizon when weakly interacting particles become nonrelativistic. In the case of HDM there is no branch with k^{-3} slope as $M_v \sim M_{\text{eq}}$.

Equation (4.7) gives only a qualitative description of the spectrum. Accurate numerical calculations of the HDM spectrum were carried out by Bond and Szalay (1983), who also provided an analytic expression to approximate the numerical results,

$$\delta_k^2 \propto k 10^{-2(k/k_v)^{1.5}}, \quad (4.8a)$$

$$k_v \approx 0.49 \Omega_0 h_{100}^2 \text{ Mpc}^{-1},$$

where $h_{100} = H_0 / (100 \text{ km s}^{-1} \text{ Mpc}^{-1})$. Another approximation of the same numerical data was suggested by Doroshkevich (1984),

$$\delta_k^2 \propto \frac{k}{(1 + k^2 R_v^2)^{12}}, \quad (4.8b)$$

$$R_v \approx 4.8 \left[\frac{m_v}{30 \text{ eV}} \right]^{-1} \text{ Mpc}.$$

Similar numerical calculations of the spectrum of density fluctuations in CDM were performed by Peebles (1982a), Blumenthal and Primack (1983), Bond and Efstathiou (1984), and Starobinsky and Sahni (1984).

There are also a few analytical approximations of these results. One of them is as follows (Peebles, 1982b, 1984a):

$$\delta_k^2 \propto k / (1 + \alpha k + \beta k^2)^2, \quad (4.9a)$$

where $\alpha \approx 24(\theta/h_{50})^2 \text{ Mpc}$, $B \approx 42(\theta/h_{50})^4 \text{ Mpc}^2$, and $\theta = T_{r,0}/2.7 \text{ K}$. Another approximation, suggested by Bond and Efstathiou (1984) in a slightly more general form, is

$$\delta_k^2 \propto \frac{k}{(1 + \alpha k + \beta k^{1.5} + \gamma k^2)^2} \quad (4.9b)$$

with $\alpha \approx 6.8 l \text{ Mpc}$, $\beta \approx 72 l^{3/2} \text{ Mpc}^{1.5}$, $\gamma \approx 16 l^2 \text{ Mpc}^2$, and $l = (\Omega h_{50}^2 \theta^{-2})^{-1}$.

The approximation proposed by Starobinsky and Sahni (1984) is

$$\delta_k^2 = \frac{1}{A^4 k^3} \frac{\ln^2(1+Bk)}{\left[1 + \frac{\ln(1+Bk)}{(Ak)^2} \right]^2}, \quad (4.9c)$$

where $A + 12.3\theta^2 \chi^{1/2} h_{50}^{-2} \text{ Mpc}$; $B = 7.3\theta^2 \chi^{1/2} h_{50}^{-2} \text{ Mpc}$; $\chi = \Omega_{\text{rel},0}/\Omega_{\gamma,0}$. This last approximation correctly reproduces the limiting cases both at $k \rightarrow 0$ and $k \rightarrow \infty$.

It is worth stressing that the transition from one stage to the other occupies a range of more than two orders of magnitude in k .

F. Decoupling epoch

At early times the temperature in the universe was so high that ordinary baryonic matter was in a completely ionized state. In the course of expansion the temperature decreased, and at about $T \approx 4000 \text{ K}$ (i.e., at $z_d \sim 1400$) atoms of hydrogen formed and the baryonic gas became practically neutral. This cosmological recombination is a very important event from the point of view of inhomogeneity growth.

Before recombination at $z > z_d$ the highly ionized baryonic gas was strongly coupled with the background radiation, which caused very high elasticity, so that the speed of sound was about the speed of light. As a result, baryon perturbations with scale less than the horizon could not grow—in other words, the Jeans scale was approximately the same as the horizon.

After recombination, neutral¹ baryonic gas decoupled from the radiation. The Jeans mass fell to about $10^6 M_\odot$, and all perturbations of larger scale could grow due to gravitational instability.

After decoupling, the amplitude of the baryonic perturbations grew rapidly to match that of the dark fluctuations (Grishuk and Zelovich, 1981).

In the case of HDM the scale of perturbations is much greater than the Jeans scale, and therefore one can neglect the temperature of the matter. In the linear regime, density perturbations of a cold medium ($T=0$ and $p=0$) grow in a self-similar manner (Doroshkevich and Zeldovich, 1964),

$$\frac{\delta\rho}{\rho} \left[\frac{\mathbf{r}}{a(t_2)}; t_2 \right] = \frac{b(t_2)}{b(t_1)} \frac{\delta\rho}{\rho} \left[\frac{\mathbf{r}}{a(t_1)}; t_1 \right],$$

where $a(t)$ is a scale factor and $b(t)$ describes the growth of the amplitude, to be discussed later.

It is not difficult to analyze the next approximation, taking into account the gas pressure in the limit

¹In this model, initially recombination proceeds in accord with the equilibrium Saha equation. Later noticeable deviations connected with the structure of hydrogen atom levels become important (Peebles, 1968; Zeldovich *et al.*, 1968). However, this is unimportant for the growth of density fluctuations.

$\lambda/\lambda_j \gg 1$ (Zeldovich, 1982b).

Let us introduce a new function $\Psi(\mathbf{r}/a, t)$,

$$\frac{\delta\rho}{\rho} = b(t)\Psi\left[\frac{\mathbf{r}}{a}, t\right],$$

and assume that it changes slowly with t . Then using the equation for linear evolution one can find

$$\frac{\partial\Psi}{\partial t} = \frac{c_s^2}{a^2}\nabla_{\mathbf{r}/a}^2\Psi,$$

where $c_s(t)$ is the speed of sound. The solution of this equation is

$$\Psi\left[\frac{\mathbf{r}}{a}, t\right] = \int K\left[\frac{\mathbf{r}}{a} - \frac{\mathbf{r}'}{a'}, \tau\right]\Psi\left[\frac{\mathbf{r}'}{a'}, t_1\right]d^3r',$$

where

$$K(\mathbf{R}, \tau) = \frac{1}{(2\pi\tau)^{3/2}}e^{-R^2/4\tau},$$

$$\tau = \int_{t_1}^t \frac{c_s^2}{a^2} \left[\frac{db}{dt}\right]^{-1} dt.$$

An important result of the study of linear evolution of density perturbations after decoupling is that both dark matter and baryonic inhomogeneities on scales larger than about $10^6 M_\odot$ enter the nonlinear regime simultaneously.

V. APPROXIMATE SOLUTION OF NONLINEAR GRAVITATIONAL INSTABILITY

We begin by discussing the nonlinear stage of gravitational instability within the HDM model.

The approximation of a cold medium (i.e., with $T=0$) is appropriate in this case, as there are practically no perturbations on scales smaller than $M_\nu \sim 2 \times 10^{15} M_\odot$ (4.3), and the Jeans mass is much less.

The growing mode of density perturbations can be described with good precision by the approximate solution (Zeldovich, 1970)

$$\mathbf{r}(\mathbf{q}, t) = a(t)[\mathbf{q} - b(t)\mathbf{s}(\mathbf{q})], \quad (5.1)$$

where \mathbf{r} are the Eulerian coordinates of the particle at time t having unperturbed Lagrangian coordinates \mathbf{q} at a time when $a=1$; $a(t)$ is a scale factor describing the Hubble expansion of the universe. It is convenient to use a normalization $a=(1+z)^{-1}$ (z is the redshift), so that $a=1$ at the present time with $z=0$. The spatial structure of the initial perturbations is described by the potential vector field

$$\mathbf{s}(\mathbf{q}) = \nabla\Phi_0(\mathbf{q}),$$

where Φ_0 is proportional to the fluctuation of the gravitational potential φ , at the linear stage which is the principal quantity to study at an early stage of inflation (Kofman and Shandarin, 1988). The density perturbations at

the linear stage are related to the vector field $\mathbf{s}(\mathbf{q})$ as $\delta\rho/\rho \propto \nabla\mathbf{s}(\mathbf{q})$. The function $b(t)$ is the growing solution for the amplitude of density fluctuations in linear theory at the matter-dominated stage. In a flat universe ($\Omega=1$), $b(t) \propto t^{2/3}$. As was pointed out in the Introduction, one can easily modify Eq. (5.1) to describe the motion of a noninteracting medium and use most of the results obtained in the first part of the paper. For instance, one can easily find an expression for density as a function of t and Lagrangian coordinates similar to Eq. (3.3),

$$\rho(\mathbf{q}, t) = \frac{\rho_0}{a^3[1-b(t)\alpha(\mathbf{q})][1-b(t)\beta(\mathbf{q})][1-b(t)\gamma(\mathbf{q})]}, \quad (5.2)$$

where α , β , and γ are again the eigenvalues of the deformation tensor $\partial s_i/\partial q_k$.

The first distinction of the approximate nonlinear theory of gravitational instability from the linear theory is that it predicts the formation of the first nonlinear objects from the high peaks of $\alpha(\mathbf{q})$ instead of $(\delta\rho/\rho)(\mathbf{q}) \propto (\alpha+\beta+\gamma)$, as in the linear theory.

In the general case of a Friedmann matter-dominated model with arbitrary Ω , the function $b(t)$ is the growing solution of the equation

$$\frac{d^2b}{dt^2} + 2\frac{da}{a}\frac{db}{dt} + 3\frac{1}{a}\frac{d^2a}{dt^2}b = 0, \quad (5.3)$$

which is well known in the linear theory of gravitational instability (Lifshitz, 1946; Lifshitz and Khalatnikov, 1963). If $\Omega \neq 1$, $b(t)$ is a rather bulky expression (see, for example, Peebles, 1980; Zeldovich and Novikov, 1983), inconvenient for analytical work. However, in open models b can be approximately written as a simple function of z ,

$$b(z) \approx \frac{b_0}{1+\omega z},$$

$$\omega = 2.5\Omega_0/(1+1.5\Omega_0), \quad (5.4)$$

which has a precision not worse than about 15%, for $0.01 \lesssim \Omega_0 \lesssim 1$.

There is a rather simple estimate for the self-consistency of the approximate solution (5.1) (Doroshkevich *et al.*, 1973). Equation (5.2) gives the density distribution as a function of t and \mathbf{q} . However, one can calculate the density distribution indirectly using the Poisson equation. To do this, let us find the acceleration field taking the second derivative of Eq. (5.1), $\mathbf{w}(\mathbf{q}, t) = d^2\mathbf{r}/dt^2$, and then evaluate the density using the Poisson equation $\bar{\rho}(\mathbf{q}, t)$. If Eq. (5.1) were an exact solution, both ways would give the same result $\rho(\mathbf{q}, t) = \bar{\rho}(\mathbf{q}, t)$. In fact they are different, since (5.1) is not the exact solution of gravitational instability. It has been shown that the self-consistent part of Eq. (5.1) can be considered as a subclass of exact solutions with restricted initial conditions (Buchert, 1988). However, Eq. (5.1) is approximately correct for generic initial conditions, and therefore ρ and $\bar{\rho}$ are close for a rather long time, even at the nonlinear

stage, when both ρ and $\bar{\rho}$ are large. While ρ and $\bar{\rho}$ are not very different, the precision of approximation (5.1) can be estimated by the dimensionless ratio

$$\Delta = \frac{\bar{\rho} - \rho}{\rho},$$

which after simple calculation can be expressed as

$$\Delta = -b^2 J_2 + 2b^3 J_3,$$

where $J_2 = \alpha\beta + \alpha\gamma + \beta\gamma$ and $J_3 = \alpha\beta\gamma$ are the invariants of the tensor $\partial s_i / \partial q_k$. It is interesting that $\Delta < 1$, even in the vicinity of the centers of pancakes and even at $\rho \rightarrow \infty$ (as well as $\bar{\rho} \rightarrow \infty$).

It is worth remembering that in spite of the formal similarity of Eq. (5.1) to inertial motion, it describes the motion of matter until it reaches the boundaries of pancakes under the action of gravity in an expanding universe. If there were no gravitational interaction (say, an imaginary medium of test particles), density perturbations would not grow in an expanding universe, as their velocities would be decreased by the expansion.

Comparison of the approximate solution with the results of direct numerical simulations under the same initial conditions have shown that at the beginning of the nonlinear stage it gives the general distribution of density very well (Doroshkevich *et al.*, 1980; Efstathiou and Silk, 1983). The approximation fails first in the regions of multistream flows. Nevertheless it remains qualitatively true for a while after the formation of pancakes. Moreover, it is worth stressing that the character of the first two singularities arising at the nonlinear stage (i.e., A_3 and A_2) is not changed in a self-gravitating medium (Roytvarf, 1987, 1988).

At present Eq. (5.1) is also used for calculation of the initial stage in numerical simulations of gravitational instability and large-scale structure formation, for which it is advantageous to start the simulation from a rather late stage when $\delta\rho/\rho \sim 0.2-0.5$, to save computational time (Doroshkevich *et al.*, 1980; Klypin and Shandarin, 1981).

If the reader has been convinced that approximation (5.1) is at least qualitatively true at the beginning of the linear stage, he or she can apply the results of preceding sections where nonlinear effects in noninteracting media were studied.

VI. GRAVITATIONAL STICKING

To discuss this effect let us return to the discussion of the evolution of a 1D sinusoidal perturbation (2.13) in a collisionless medium:

$$x(t, q) = q - b(t) \sin q.$$

Before overshooting occurs, the density is given by

$$\rho(q, t) = \frac{\rho_0}{a^3 [1 - b(t) \cos q]}, \tag{6.1}$$

where ρ_0 is the mean density when $a=1$, a is the scale factor, and thus ρ_0/a^3 is the mean density at t . It turns out that in 1D both (5.1) and (6.1) are exactly true until the formation of the first singularity.

Later Eq. (5.1) becomes progressively worse at describing quantitatively the motion of matter; however, it continues to be qualitatively correct for a while. The extrapolation of Eq. (5.1) predicts very fast growth of the thickness of the pancake, but direct numerical simulations (Doroshkevich *et al.*, 1980; Melott, 1982a, 1982b, 1983a; Kotok and Shandarin, 1987), as well as theoretical analysis (Dekel, 1983; Filmore and Goldreich, 1984), have shown that the thickness increases much more slowly with time (Fig. 13). The comparison is made at equal values of a (in an expansion universe) and t (in the case of a noninteracting medium). Then, at about $a=2.4$ (the formation of the first singularity takes place at $a=1$), qualitative differences from a noninteracting medium arise. In a gravitating medium a region of five-stream flows originates. It turns out that the gravitational attraction does not allow the streams moving in opposite directions to go too far. The particles slow down and then start moving in the opposite direction. As a result the thickness of the pancake grows relatively slowly in comoving coordinates. The same is also true in gas systems (Doroshkevich and Shandarin, 1973; Shapiro *et al.*, 1983).

Thus in a gravitating medium even without collisions there is effective sticking after the formation of multistream flows. Another illustration of this effect is Fig. 14 (Doroshkevich *et al.*, 1980), where, at some moment of time after overshooting, the dependence of the Lagrangian coordinate q on the Eulerian one x is shown. It is evident that in the case of physical sticking into an infinitely thin layer, instead of a wavy curve there would be a vertical line.

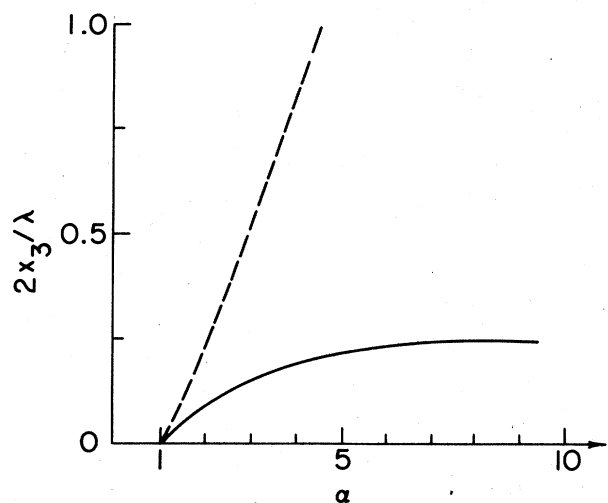


FIG. 13. Growth of pancake thickness with a in gravitating matter: solid line, a 1D numerical simulation; dashed line, an extrapolation of Zeldovich's solution. The sizes are given in terms of the wavelength.

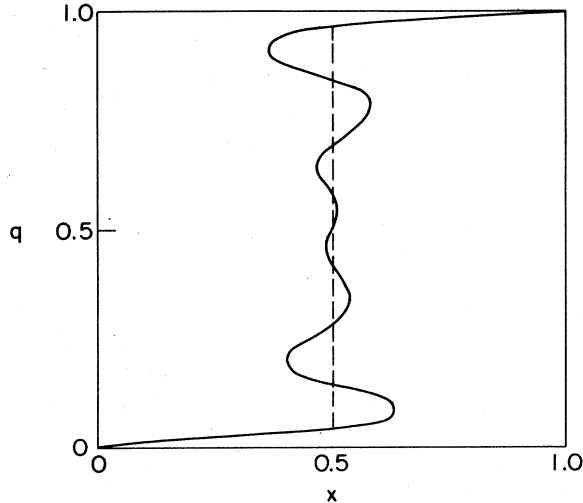


FIG. 14. Illustration of “gravitational sticking.” The dependence of a Lagrangian coordinate on an Eulerian one is shown in gravitating collisionless matter at an advanced nonlinear stage. The positions of singularities coincide with points where $\partial v / \partial x = \infty$. At these points the number of streams also increases by 2 (1D numerical simulation). The dashed line shows the dependence $q(x)$ for sticky matter.

As we shall see in the next section, this effect permits one to use the Burgers equation to extend the analytic approximate solution to later nonlinear stages. Finally it is worth stressing that the effect of gravitational sticking in collisionless media has also been observed in 2D and 3D numerical experiments (Doroshkevich *et al.*, 1980; Klypin and Shandarin, 1981).

VII. THE LATE STAGE OF NONLINEAR GRAVITATIONAL INSTABILITY

What happens to pancakes and other structures later? The question seems to be somewhat academic for the HDM model, as it concerns the future. However, in the CDM model the first pancakes (formed, by the way, only in the dark matter component) are of very small sizes, as mentioned above; the formation of large-scale structure is the result of later nonlinear evolution of density inhomogeneities.

In this section we describe an attempt to extend the nonlinear approximate solution (5.1) using the additional idea of gravitational sticking discussed above (Gurbatov and Saichev, 1984; Gurbatov *et al.*, 1984, 1985, 1989; Shandarin, 1987, 1988; Kofman and Shandarin, 1988). Mathematically this sticking is described by the well-known Burgers equation (Burgers, 1948, 1974).

First we show how the Burgers equation comes out of the familiar equations describing the evolution of density inhomogeneities in the hydrodynamical approximation. We need not concern ourselves with a hydrodynamic description of collisionless dark matter, as it is cold, and

therefore thermal velocity dispersion hardly influences the density distribution. On the other hand, the Burgers equation does not lead to multistream flows. In the frame of this approximation we have to neglect the inner structure of pancakes and of other objects.

As before we shall consider the evolution of density inhomogeneities in coordinates comoving with the Hubble expansion of the universe,

$$\mathbf{x} = \mathbf{r} / a(t) .$$

Instead of the full velocity we shall use only a part called the peculiar velocity,

$$\mathbf{v} = \mathbf{u} - \frac{\dot{a}}{a} \mathbf{r} = a \, d\mathbf{x} / dt .$$

In these variables the system of equations describing the evolution of density inhomogeneities is (see, for example, Peebles, 1980)

$$\begin{aligned} \frac{\partial \rho}{\partial t} + 3 \frac{\dot{a}}{a} \rho + \frac{1}{a} \nabla_x \rho \mathbf{v} &= 0 , \\ \frac{d\mathbf{v}}{dt} + \frac{\dot{a}}{a} \mathbf{v} &= - \frac{1}{a} \nabla_x \Phi , \\ \nabla_x^2 \Phi &= 4\pi G a^2 [\rho(\mathbf{x}, t) - \bar{\rho}(t)] . \end{aligned} \tag{7.1}$$

Here the index x indicates that the spatial derivatives are taken with respect to x , $\Phi(\mathbf{x}, t)$ is the perturbation of gravitational potential that is generated by density perturbation $[\rho(\mathbf{x}, t) - \bar{\rho}(t)]$, and $\bar{\rho}$ is the mean density.

Let us use the approximate solution (5.1) to calculate explicitly the velocity

$$\mathbf{v} = a \dot{\mathbf{b}} \mathbf{s}(\mathbf{q}) \tag{7.2}$$

and gravitational acceleration field

$$\frac{d\mathbf{v}}{dt} = (a \ddot{\mathbf{b}} - a \dot{\mathbf{b}} \dot{\mathbf{s}}) \mathbf{s}(\mathbf{q}) . \tag{7.3}$$

Expressing $\mathbf{s}(\mathbf{q})$ from Eq. (7.2) and putting in into Eq. (7.3) we get

$$\frac{d\mathbf{v}}{dt} = \frac{\dot{a}}{a} \mathbf{v} + \frac{\ddot{\mathbf{b}}}{\dot{\mathbf{b}}} \mathbf{v} . \tag{7.4}$$

Now let us introduce new variables: b instead of t and $\vartheta = \mathbf{v} / (a \dot{\mathbf{b}})$ instead of \mathbf{v} . The second equation in system (7.1) becomes (Shandarin, 1988)

$$\frac{\partial \vartheta}{\partial b} + (\vartheta \nabla_x) \vartheta = 0 . \tag{7.5}$$

Using $\eta = a^3 \rho$ instead of ρ we get the system

$$\begin{aligned} \frac{\partial \eta}{\partial b} + \nabla_x (\eta \vartheta) &= 0 , \\ \frac{\partial \vartheta}{\partial b} + (\vartheta \nabla_x) \vartheta &= 0 , \end{aligned} \tag{7.6}$$

instead of the original one (7.1). The second equation does not depend on η and has an evident solution connecting Lagrangian and Eulerian coordinates of particles,

$$\mathbf{x} = \mathbf{q} + b \mathfrak{D}_0(\mathbf{q}) . \tag{7.7}$$

This solution, except for the notation, coincides with Eq. (5.1), which is not surprising at all, as transforming Eq. (7.1) into (7.6) we have used the acceleration field determined from (5.1). Thus the solution of the system (7.6) is physically equivalent to Eq. (5.1).

The next step consists in a modification of the second equation of system (7.6), inserting the term $\nu \nabla_x^2 \mathfrak{D}$ modeling artificial viscosity,

$$\frac{\partial \mathfrak{D}}{\partial b} + (\mathfrak{D} \nabla_x) \mathfrak{D} = \nu \nabla_x^2 \mathfrak{D} . \tag{7.8}$$

Assuming that the viscosity coefficient ν is small, $\nu \rightarrow 0$, let us consider what has changed with the medium motion due to this term. At $\nu \rightarrow 0$ the viscosity influences the motion nowhere except at the places of sharp velocity changes. They are the regions of pancake formation. This artificial term prevents the formation of multistream flows. Instead of layers, thin sheets arise. We note that the smaller ν is, the thinner the sheets are.

The essential advantage of the Burgers equation is that it has an exact solution for the potential velocity field. Generalization of the solution from 1D to 3D was carried out by Kuznetsov and Rozhdestvensky in 1961. Using the Hopf-Cole substitution in vector form (cf. Sec. II.B.3)

$$\mathfrak{D}_i(\mathbf{x}, b) = -2\nu \frac{\partial}{\partial x_i} \ln U(\mathbf{x}, b)$$

one gets a linear diffusion equation

$$\frac{\partial U}{\partial b} = \nu \nabla_x^2 U$$

with a known general solution. Returning to the velocity field we have

$$\mathfrak{D}(\mathbf{x}, b) = \frac{\int \frac{\mathbf{x} - \mathbf{q}}{b} \exp \left[-\frac{G(\mathbf{x}, \mathbf{q}, b)}{2\nu} \right] d^3q}{\int \exp \left[-\frac{G(\mathbf{x}, \mathbf{q}, b)}{2\nu} \right] d^3q} , \tag{7.9}$$

where

$$G(\mathbf{x}, \mathbf{q}, b) = \Phi_0(\mathbf{q}) + \frac{(\mathbf{x} - \mathbf{q})^2}{2b} \tag{7.10}$$

and $\Phi_0(\mathbf{q})$ is the potential of the initial velocity field,

$$\mathfrak{D}(\mathbf{q}) = \nabla_q \Phi_0(\mathbf{q}) . \tag{7.11}$$

In analogy to the 1D case, the main input into integrals at given a and \mathbf{x} comes from the vicinity of the absolute negative minimum of $G(\mathbf{x}, \mathbf{q}, b)$ taken as a function of \mathbf{q} .

There is a convenient geometrical procedure for finding the velocity field in Eulerian coordinates based on solution (7.9). It can be shown that the coordinates \mathbf{q} of the absolute minimum of $G(\mathbf{x}, \mathbf{q}, b)$ [Eq. (7.10)] are the coordinates of the point where the hypersurface $\Phi_0(\mathbf{q})$ is touched by a 3D paraboloid

$$p(\mathbf{x}, \mathbf{q}, b) = -\frac{(\mathbf{x} - \mathbf{q})^2}{2b} + H \tag{7.12}$$

when H grows from $-\infty$.

Considering potential $\Phi_0(\mathbf{q})$ as a statistically homogeneous and isotropic smooth Gaussian random field, let us qualitatively describe the evolution of the velocity field with time. We note that the condition of smoothness requires that the spectrum of $\Phi_0(\mathbf{q})$ decrease steeply enough at short wavelengths (i.e., at $k \rightarrow \infty$).

The curvature of the paraboloid $p(\mathbf{x}, \mathbf{q}, b)$ changes with time. At small b the paraboloid is very narrow, but later it becomes more shallow.

When b is small the paraboloid can touch every point of $\Phi_0(\mathbf{q})$ in such a way that it intersects $\Phi_0(\mathbf{q})$ at no other points. This is the linear stage of the evolution of density perturbations. At this stage there is a one-to-one correspondence between \mathbf{q} (i.e., the contact point) and \mathbf{x} (i.e., the top of the paraboloid).

Thus it is possible to find the velocity field $\mathfrak{D}(\mathbf{x}, b)$ in E space, since at a point $\mathbf{x} = \mathbf{q} + b \mathfrak{D}_0(\mathbf{q})$ the velocity is $\mathfrak{D}(\mathbf{x}, b) = \mathfrak{D}_0(\mathbf{q})$.

However, later points of \mathbf{x} appear where the paraboloid $p(\mathbf{x}, \mathbf{q}, b)$ touches $\Phi_0(\mathbf{q})$ at several points of \mathbf{q} (generally speaking at different values of H). It occurs when in the collisionless case multistream flows would arise, that is, at the nonlinear stage of evolution. From Eqs. (7.9), (7.10), and (7.12) it can be seen that only contact points at the lowest values of H must be considered. Geometrically this means that only points \mathbf{q} where the paraboloid $p(\mathbf{x}, \mathbf{q}, b)$ touches the hypersurface $\Phi_0(\mathbf{q})$ without interacting are allowed. The other points have stuck in sheets previously.

The positions of the paraboloid where it has two contact points with $\Phi_0(\mathbf{q})$ at the same H are of particular interest. In such a position the paraboloid indicates with its vertex the points lying on sheets of infinite density (at $\nu \rightarrow 0$). The velocity field breaks the continuity at these points. These sheets originate as small pieces of surfaces, but later they grow and join with others, forming a cellular structure. The ribs of the structure are the set of top points of the paraboloid where it touches the hypersurface $\Phi_0(\mathbf{q})$ at three points simultaneously. In turn the ribs join in knots, which are those points of paraboloids' tops which touch $\Phi_0(\mathbf{q})$ in four points simultaneously.

According to the sticking model, the matter that sticks into sheets partly reduces the velocity component normal to the sheet but continues to move along the sheet. It moves into the ribs and then along the ribs until it comes to the knots. Qualitatively similar predictions are given by the model based on the process known as Voronoi tessellation (Icke and van de Weygaert, 1987). The model looks quite promising, but unfortunately in the present form it ignores both the difference in expansion rates of voids and the evolution of their sizes with time.

The sticking model in its present form cannot describe the inner structure of dense regions, sheets, ribs, or knots. It is designed to provide the masses, positions, and velocities of knots and other elements of the struc-

ture (Gurbatov and Saichev, 1984; Gurbatov *et al.*, 1984, 1985, 1989). The first results of 2D numerical calculations (Kofman *et al.*, 1989) show good qualitative agreement of the sticking model with N -body simulations. In the course of time the fraction of mass that has not entered dense regions, that is, that remained in voids, grows smaller, and the total mass contained in knots becomes greater. The knots and other elements of the structure move and merge into more massive knots. This stage naturally describes the well-known hierarchical clustering process (see, for example, Peebles, 1980). Physical analysis of the process of merging of two clusters of collisionless particles (White and Rees, 1978; McGlynn and Fabian, 1984) has shown that they quickly lose their identities and become a single cluster. The same is true in the case of merging of many clusters (Carnevali *et al.*, 1981). Thus the sticking model is qualitatively correct in its description of this process.

Let us return to our geometrical procedure of inserting paraboloids into the hypersurface $\Phi_0(\mathbf{q})$. It is quite evident that at large $b(t)$, when the paraboloid is very shallow, it touches $\Phi_0(\mathbf{q})$ only in the vicinities of the deepest minima. Therefore all information about integral parameters of knots (i.e., their masses, coordinates, and velocities) can be inferred from distribution of minima in the initial potential $\Phi_0(\mathbf{q})$.

At present the statistical properties of peaks of a scalar Gaussian random function have been carefully studied from the point of view of large-scale structure formation, but in a different context (Doroshkevich, 1970; Peacock, and Heavens, 1985; Bardeen *et al.*, 1986; Couchman, 1987). At the linear stage, the potential $\Phi_0(\mathbf{q})$ and density perturbations $\delta\rho/\rho$ relate as

$$\frac{\delta\rho}{\rho} \propto \frac{\partial^2 \Phi_0(\mathbf{q})}{\partial q_j^2},$$

which in particular leads to the following relation between the spectra:

$$\Delta_k^2 \propto k^{-4} \delta_k^2.$$

Here Δ_k^2 is the spectrum of the potential $\Phi_0(\mathbf{q})$, and δ_k^2 is as usual the spectrum of $\delta\rho/\rho$ [see Eq. (9.1)]. Naturally the influence of long waves is stronger in Δ_k^2 than in δ_k^2 .

The beginning of the nonlinear stage is characterized by formation of sheets and ribs. At this stage the growth of the typical knot mass is determined mostly by the process of mass flow from sheets and ribs into knots. In later stages most of the mass is already in the knots, and the growth of the characteristic mass of the knots is the result of merging of smaller ones.

Theoretically it is interesting that in spite of the fact that the knots are a point mass concentration [at $v \rightarrow 0$ in Eq. (7.8)], they can effectively collide and merge in accord with the sticking model. This property is connected with the potential character of the motion.

Now let us discuss the growth of the typical mass of knots at the late nonlinear stage in the case of a simple

power-law spectrum of the linear density perturbation

$$\delta_k^2 \propto k^n \quad \text{at } k \rightarrow 0. \quad (7.13)$$

This of course means that

$$\Delta_k^2 \propto k^{n-4}.$$

In the case of rather flat spectra $-1 \leq n \leq 1$, the characteristic mass of clumps m_{cl} grows as

$$m_{cl}(b) \propto b^{6/(n+3)}, \quad (7.14)$$

in complete accord with the prediction of linear theory (Peebles, 1980).

However, at $n > 1$ the sticking model predicts a different law for mass growth,

$$m_{cl}(b) \propto b^{3/2}, \quad (7.15)$$

independently of n (Gurbatov *et al.*, 1984, 1985, 1989).

On the other hand, the linear theory of hierarchical clustering gives the same rate (7.14) for $1 \leq n \leq 4$. Earlier it was found (Press and Schechter, 1974; Doroshkevich and Zeldovich, 1975) that due to nonlinear generation of long-wavelength perturbations (*even* at the *linear stage*, i.e., while $\delta\rho/\rho < 1$) with the spectrum $\delta_k^2 \propto k^4$, there is a limit law for the growth of a typical cluster mass $m_{cl} \propto a^{6/7}$ at $n > 4$. Thus for large spectrum indices $n > 1$ there is a disagreement between the predictions of the linear theory of hierarchical clustering and the sticking model based on the Burgers equation.

It is interesting that, according to the sticking model, the limit law for the mass growth depends on the dimensionality of the space,

$$m_{cl}(b) \propto b^{d/2} \quad \text{at } n \geq n_{cr} = 4 - d, \quad (7.16)$$

where $d=1,2,3$ is the dimensionality of the space.

In 1D numerical simulations (Kotok and Shandarin, 1988), it was observed that there is nonlinear generation of the long-wavelength part of the spectrum having the slope $\delta_k^2 \propto k^4$. This is in perfect accord with early results (Press and Schechter, 1974; Doroshkevich and Zeldovich, 1975), but the growth rate of this part of the spectrum confirms the prediction (7.16) for the 1D case.

The sticking model indicates a more complicated process of clustering in the case of negative spectrum indices at $n < -1$ in Eq. (7.13). The reason is that the statistical characteristics of the potential $\Phi_0(\mathbf{q})$ peaks are controlled by the long-wavelength part of the spectrum $\Delta_k^2 \propto k^{-4} \delta_k^2$. At $n < -1$ the spatial distribution of high peaks of $\Phi_0(\mathbf{q})$ cannot be considered homogeneous. If one assumes that spectrum $\delta_k^2 \propto k^n$ ($n < -1$) turns over at some $k = k_b$ bearing $\delta_k^2 \propto k^m$ with $m > -1$ at $k < k_b$, then the clustering process in the range $k > k_D$ will depend on the scale k_b .

VIII. NUMERICAL SIMULATIONS

Numerical simulations of nonlinear gravitational instability in collisionless matter are of great importance both

for understanding the physical process and for the study of large-scale structure formation. At present numerical simulations are widely used to model individual objects like galaxies and clusters of galaxies. Here we briefly discuss simulations of large-scale structure as a whole.

The characteristic feature of numerical simulations of large-scale structure is that they are based on collisionless models. Gas dynamics and thermal processes are essential on the scale of galaxies or smaller. The structure of rich clusters and superclusters of galaxies depends mostly on gravitational processes in the collisionless dark component. However, 1D gas dynamic simulations have been carried out within the framework of a baryon-dominated universe or of the HDM model (Doroshkevich and Shandarin, 1973; Bond *et al.*, 1983; Shapiro *et al.*, 1983).

A general scheme for numerical simulations of gravitational instability in collisionless matter is as follows. A model consists of N bodies generally of equal masses that move in the gravitational field generated by their own distribution. There are two principal steps: (1) calculation of the forces acting on every particle and (2) calculation of new positions and velocities that the particles acquire in a small interval of time due to action of those forces. Repeating these steps many times one can follow the evolution of the system.

There are three methods for calculation of forces used at present: (1) PP (particle-particle) scheme, (2) CIC (cloud in cell) or PM (particle-mesh) scheme, and (3) P³M (particle-particle/particle-mesh) scheme.

In the PP method the force acting on particle i is calculated as a sum of forces exerted by other particles,

$$\mathbf{F}_i = Gm_i \sum_{j \neq i} \frac{m_j(\mathbf{r}_j - \mathbf{r}_i)}{[(\mathbf{r}_j - \mathbf{r}_i)^2 + \epsilon^2]^{3/2}}, \quad (8.1)$$

where m_i is the mass of the i th particle, G is the gravitational constant, and ϵ is the length of softening of force at small distances introduced to avoid the calculation of arbitrarily large forces between close particles. The main disadvantage of this method is that it takes a great deal of time to calculate the forces; therefore typical numbers of particles in the simulations are only several thousand.

Most studies of the hierarchical clustering scenario have been done on the basis of this technique (Fall, 1978; Aarseth *et al.*, 1979; Efstathiou, 1979; Efstathiou *et al.*, 1979; Gott *et al.*, 1979; Turner *et al.*, 1979; Gott, 1980) as well as some investigations in the pancake scenario (Frenk *et al.*, 1983; White *et al.*, 1983, 1984; Dekel, 1984, 1985; Dekel and Aarseth, 1984).

Another method for calculating gravitational forces also actively used in the simulation of large-scale structure formation is the CIC or PM technique. It was first used for numerical study of collective phenomena in a rarefied plasma (Eastwood, 1976). In this method a regular spatial mesh is introduced to calculate a smooth density distribution, which in turn is used to calculate the gravitational potential. Usually the potential is computed by using a fast Fourier transform (FFT). Then the

gravitational forces are calculated by means of numerical differentiation and interpolation. The Fourier transform assumes periodic boundary conditions that effectively simulate infinite space. It should be noted that the number of particles need not be equal to the number of mesh zones. The optimal choice of differentiation scheme allows the spatial resolution of 1–2 mesh periods (Melott, 1986). The PM method is considerably faster than the PP method, and typically simulations are performed with 32^3 or 64^3 particles and a comparable number of mesh zones.

In cosmology this technique was first introduced by Doroshkevich *et al.* (1980) for analysis of 1D and 2D models. Later 3D models were also developed (Klypin and Shandarin, 1981; Shandarin 1983a). At present it is widely used for analysis of different scenarios of large-scale structure formation (Centrella and Melott, 1983; Melott, 1983b; Melott *et al.*, 1983; Miller, 1983; Bouchet *et al.*, 1985; Hansel *et al.*, 1985; Melott and Scherrer, 1987; Centrella *et al.*, 1988).

So far, the best spatial resolution has been achieved within the framework of the P³M method. This method, which uses both the FFT technique for the long-range gravitational field and the interaction with a few nearest-neighbor particles, is calculated directly as in the PP method (Efstathiou and Eastwood, 1981). A detailed comparison of PM and P³M methods was made by Efstathiou *et al.* (1985); see also Centrella *et al.* (1988) and Melott *et al.* (1988).

Perhaps the most important parameter characterizing the capabilities of a numerical model is the ratio between the largest and the smallest scale it reliably deals with. Another very important parameter, partly related to this, is the number of particles in the simulation. The record spatial range covered, 2–2.5 orders of magnitude in length scale, was achieved in P³M simulations (Efstathiou *et al.*, 1985); recently even $\lambda_{\max}/\lambda_{\min} \approx 600$ has been reported (Davis, 1987).

Unfortunately even this range cannot cover the range of large-scale structure, say, between galaxies (~ 10 kpc) and the largest observed inhomogeneities (~ 100 – 300 Mpc) (Kopylov *et al.*, 1984; Batuski and Burns, 1985; Tully, 1987). Taking into account that to obtain reliable statistic of large-scale objects one needs probably even larger simulation “boxes,” it becomes clear that the results of numerical simulations must be interpreted very carefully.

The essential feature of the evolution of inhomogeneities in collisionless dark matter is the extreme weakness of the process of pair relaxation caused by the enormous number of particles. For instance, if the mass of rich clusters consists mostly of neutrinos with a mass of about 30 eV then the total number of neutrinos is about 10^{80} . As was mentioned above, the typical number of particles in numerical simulations is about 10^5 , which is incomparably less. Thus one must take special precautions to avoid an artificial effect of pair relaxation in the numerical simulations. From this point of view, the PM method is the safest.

Many numerical simulations have been carried out with an initial Poisson distribution of particles inside a sphere. In most cases initial peculiar velocities were taken equal to zero. This initial state supposes that the initial density perturbation spectrum is flat: $\delta_k^2 \propto k^0$ or $\delta N/N \propto N^{-1/2}$. Moreover, it assumes that there were some nonlinear perturbations on small scales $R < \bar{n}^{-1/3}$ from the very beginning.

A more flexible method for generating the initial state, proposed by Doroshkevich *et al.* (1980) is based on the approximate solution (5.1). A quasihomogeneous distribution of particles is generated by putting them on a regular cubical mesh. Then the coordinates and velocities are perturbed by using Eq. (5.1), which generates the growing mode of density perturbation with a chosen spectrum and amplitude. Another advantage of this technique is the possibility of starting with a relatively large initial amplitude of density perturbations ($\delta\rho/\rho \sim 0.2-0.5$), since approximation (5.1) has a very good precision at this stage. As a result one saves computational time.

Up to now, numerical simulations have been performed to study different aspects of large-scale structure formation mostly in HDM and CDM scenarios based on the assumption that the initial perturbations are Gaussian in character (references mentioned above). However, first attempts have been made to simulate large-scale structure formation in the framework of the explosion scenario (Saarinen *et al.*, 1987) and in the model of cosmic strings (Melott and Scherrer, 1987).

The development of numerical simulations has brought the study of large-scale structure formation to a qualitatively different level. At present in many cases the results of numerical simulations provided the decisive arguments

against some models suggested to explain large-scale structure formation. The reason is that only by means of numerical simulations can one quantitatively compare the predictions of the model with the observational data.

In addition, numerical simulations have provided interesting new results concerning nonlinear processes in self-gravitating systems.

First they have confirmed the theoretical conclusion that structure in a density distribution having the appearance of irregular cells or filaments naturally arises at the nonlinear stages if the spectrum of the linear density perturbations falls off steeply enough with decreasing wavelength. Within the class of power-law spectra a falloff steeper than k^{-1} is probably required.

2D and 3D numerical simulations have shown that pancakes and filaments (Fig. 15) that formed at the beginning of the nonlinear stage in HDM models remain thin compared to their diameters. Their distortion with time is caused by matter motions along pancakes into filaments, and later along the filaments into clumps.

In fact, the idea of cellular structure in the density distribution originated on the basis of the numerical simulations made by one of the authors (S.S.) in 1975. The first picture of 2D nonlinear structure was published in a review by Doroshkevich *et al.* (1976).

Numerical simulations have also shown that pancakes, filaments, and the whole cellular network structure exist only at an intermediate epoch. Finally, practically all the mass becomes concentrated in separate clumps, which increase in mass due to continuous merging.

IX. STATISTICAL ANALYSIS OF LARGE-SCALE STRUCTURES

The essential feature of the structures discussed above is that they arise from a random Gaussian field of small density (and/or velocity) perturbations. One cannot in principle obtain information about cosmological density fluctuations at the linear stage in the region corresponding to that observed at present. Perhaps in a few years radio astronomers will succeed in piecing together a 2D map of the microwave background temperature distribution in the sky. This would enable us to estimate the density perturbations $\delta\rho/\rho$ at $z_d \sim 10^3$ with much better confidence than now, but only in the regions where galaxies cannot be observed at present. Thus we come to the conclusion that the only relation connecting initial (linear) density fluctuations with observed structures in the galaxy distribution is of statistical character (for detailed discussion see Sazhin, 1985; Zabolin and Naselskii, 1985; Bond and Efstathiou, 1987; Vittorio and Juszkewicz, 1987).

Recently many statistical approaches have been suggested, describing the large-scale structure of the universe to supporting or rejecting various theories proposed to explain the formation of this structure. To discuss all of them one would need to write an additional review that probably would be of length exceeding the

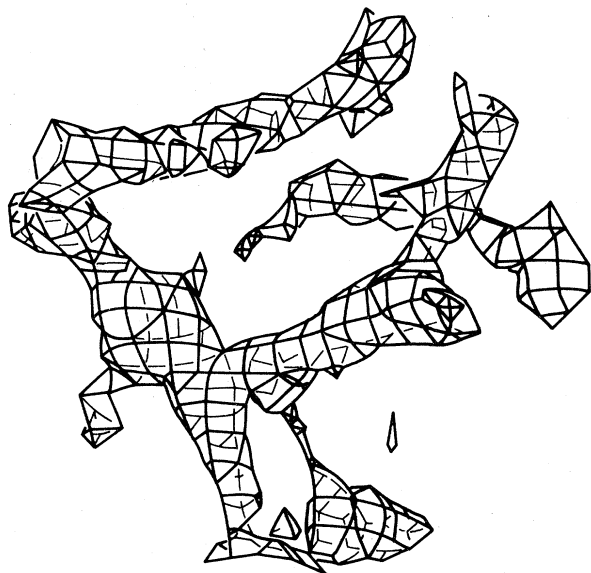


FIG. 15. The level surface $\rho \approx 2.5\bar{\rho}$ at the early nonlinear stage in a gravitating collisionless medium (3D numerical simulation).

present one. Therefore we have chosen only a couple of approaches to illustrate the problems arising in this field.

One of the methods is the very-well-known correlation analysis, whose application to large-scale structure formation has been extensively elaborated, primarily by Peebles and his collaborators (see Peebles, 1980, and references therein). At present it has become a routine test for any theory of large-scale structure formation.

The second is a statistical technique based on cluster analysis, often referred to as precolation analysis. The importance of this method for the problem has been emphasized by the authors (Zeldovich, 1982a; Shandarin, 1983b; Shandarin and Zeldovich, 1983).

In discussing both methods we intend only to give the main ideas; as we have pointed out, the problem of statistical analysis of large-scale galaxy distribution warrants a much more detailed discussion.

A. Correlation analysis

At linear stages the density perturbations are assumed to be a random Gaussian field and therefore the full statistical information about them is contained in the spectrum $\delta_k^2 \equiv \langle |\delta_k|^2 \rangle$, where

$$\delta_k = \frac{1}{V_u} \int_{V_u} \frac{\delta\rho}{\rho}(\mathbf{x}) e^{i\mathbf{k}\mathbf{x}} d^3x. \quad (9.1)$$

Here V_u is a large volume in which the distribution can be considered statistically homogeneous. It is important that δ_k have statistically independent phases if $\delta\rho/\rho$ is a Gaussian field. The other statistically equivalent characteristic of Gaussian random fields is a two-point correlation function $\xi(x)$,

$$\xi(x) = \left\langle \frac{\delta\rho}{\rho}(\mathbf{x}_1) \frac{\delta\rho}{\rho}(\mathbf{x}_1 + \mathbf{x}) \right\rangle, \quad (9.2)$$

which is related to δ_k by means of the Fourier transform

$$\xi(x) = \frac{V_u}{(2\pi)^3} \int \delta_k^2 e^{-i\mathbf{k}\mathbf{x}} d^3k. \quad (9.3)$$

Clearly the reverse is also true,

$$\delta_k^2 = \frac{1}{V_u} \int \xi(x) e^{i\mathbf{k}\mathbf{x}} d^3x \quad \text{at } k \neq 0, \quad (9.4)$$

$$\delta_0^2 = \frac{1}{\bar{n}V_u} + \frac{1}{V_u} \int \xi(x) d^3x.$$

For point distributions like the distribution of galaxies in space, the right-hand side of Eq. (9.4) acquires the additional evident term $1/(\bar{n}V_u)$, where \bar{n} is the mean density of pointlike objects.

The beginning of the nonlinear stage is characterized by the appearance of pancakes, filaments, and compact clusters. This phenomenon is known as intermittency, and with its advent the density perturbations are no longer Gaussian. The phases in the Fourier transform (9.1) cease to be statistically independent. In this case neither the spectrum nor the correlation function is a sta-

tistically complete description of the density distribution. Moreover, there is no one-to-one correspondence between the spatial density distribution and its spectrum. By adjusting the phases one can get quite different (by visual appearance) spatial distributions with the same spectrum δ_k^2 . Therefore at this stage the two-point correlation function $\xi(x)$ also does not contain the full statistical information about such random fields. In principle one needs correlation functions of higher orders: three-point, four-point, etc. The full (infinite) set of these functions does contain all statistical characteristics of an arbitrary random field. However, from the practical point of view, dealing with a function of many variables is not a very pleasant job unless it has a trivial structure. Therefore correlation functions of orders higher than three are rarely used (however, see, for example, Peebles, 1980).

In practice the situation is not all that bad. It turns out that obtaining even a two-point correlation function in the theoretical models that reasonably matches the observational one is very difficult. Therefore in contemporary cosmology any theory suggested to explain large-scale structure formation must agree with the correlation properties of the observational galaxy distribution. The most comprehensive discussion of these questions known to the authors is given in the book by Peebles (1980) and in the review by Fall (1979). Taking this into account we give just a short summary of results and problems that have to be solved.

The two-point correlation function $\xi(r)$ for pointlike objects (sometimes they can be galaxies or even rich clusters of galaxies) is

$$\delta p = \bar{n}^2 [1 + \xi(r)] \delta V_1 \delta V_2, \quad (9.5)$$

where δp is the probability of finding simultaneously two objects (say, galaxies) in two small volumes δV_1 and δV_2 separated by distance r ; \bar{n} is the mean number of objects per unit volume. A similar equation defines the three-point correlation function $\zeta(r_{12}, r_{23}, r_{31})$,

$$\delta p = \bar{n}^3 [1 + \zeta(r_{12}) + \zeta(r_{23}) + \zeta(r_{31}) + \zeta(r_{12}, r_{23}, r_{31})] \delta V_1 \delta V_2 \delta V_3, \quad (9.6)$$

or higher-order correlation functions.

There is one specifically cosmological problem for the calculation of correlation functions. To evaluate them one needs to measure the galaxy distance. At present, most distances of galaxies are estimated using the Hubble relation $u = H_0 r$, where u is the radial velocity of a galaxy, r its distance, and H_0 the Hubble constant. This method suffers principally from irreducible errors caused by the peculiar velocities of galaxies. In this connection one must remember that the inhomogeneous distribution of galaxies in space is caused by their peculiar motions, i.e., motions additional to their Hubble motions.

The results of numerous estimations of galaxy correlation functions (e.g., Totsuji and Kihara, 1969; Davis and Peebles, 1983; Einasto *et al.*, 1984) can be briefly summarized as follows:

$$\xi_g(r) = \left(\frac{r}{r_g} \right)^{-\gamma} \quad \text{with } r_g \approx 10h_{50}^{-1} \text{ Mpc and } \gamma \approx 1.8, \quad (9.7)$$

in the range

$$0.2h_{50}^{-1} \text{ Mpc} \lesssim r \lesssim 20h_{50}^{-1} \text{ Mpc}$$

at $r \gtrsim 20h_{50}^{-1} \text{ Mpc}$, $|\xi_g| < 0.1$ (Davis and Peebles, 1983).

The three-point correlation function $\xi(r_{12}, r_{23}, r_{31})$ [Eq. (9.6)] can be approximated with rather good precision by the equation

$$\xi(r_{12}, r_{23}, r_{31}) \approx Q[\xi_g(r_{12})\xi_g(r_{23}) + \xi_g(r_{23})\xi_g(r_{31}) + \xi_g(r_{31})\xi_g(r_{12})], \quad (9.8)$$

with $Q \approx 1$ (Davis and Peebles, 1983).

The first surprise is that $\xi_g(r)$ is well described by a single power law, both in $\xi_g \gg 1$ and in $\xi_g < 1$ regions. However, one might think that the former is determined by nonlinear effects and the latter is connected with the type of initial density perturbations spectrum.

Another surprising fact emerges when the correlation function of rich clusters is taken into account. It turns out that it has the same power-law form, but with the correlation scale r_c (distance, at which $\xi = 1$) five times greater,

$$\xi_c(r) \approx \left(\frac{r}{r_c} \right)^{-\gamma}, \quad (9.9)$$

with $r_c \approx 50h_{50}^{-1} \text{ Mpc}$ and $\gamma \approx 1.7-1.8$. However, this takes place in a different range of scales,

$$10h_{50}^{-1} \text{ Mpc} \leq r \leq 150h_{50}^{-1} \text{ Mpc}.$$

Although the cluster correlation function is much larger than that of galaxies, as was discovered many years ago (Hauser and Peebles, 1973), the possibility of its approximation by a power law was found only recently (Bahcall and Soneira, 1983; Klypin and Kopylov, 1983; Bahcall *et al.*, 1986).

A very interesting suggestion was made by Kaiser (1984) to explain the difference between galaxy and cluster correlation functions. He pointed out that if some random Gaussian field Φ has correlation, then the correlations between peaks of the field will be stronger. Moreover, the higher the peaks the stronger the correlation. Numerical simulations of nonlinear gravitational instability have qualitatively confirmed this effect; they have failed, however, to explain the observed difference between r_g (9.7) and r_c (9.9) (Shandarin and Klypin, 1984; Barnes *et al.*, 1985). A possible explanation of the disagreement between the theoretical prediction and the numerical results was proposed by Coles (1986).

On the other hand, evidence has appeared (Einasto *et al.*, 1986) that the galaxy correlation radius r_g grows with the volume studied. If this result (still unconfirmed by other astronomers) is true, it at least reduces the discrepancy between r_g and r_c .

B. Percolation analysis

An immediate visual impression of the light distribution in optical experiments (Figs. 10 and 11), density distribution in 2D (Fig. 12), or density distribution in 3D (Fig. 15) is that the regions of high density form a single connected system. Similar ideas arise if one observes the galaxy distribution in a thin slice (Fig. 1). However, one would wish to confirm intuitive impressions by some quantitative characteristics. One of the most appropriate techniques sensitive to such structures seems to be percolation analysis.

At present, percolation theory is used in many branches of physics, although mainly for purposes other than pattern recognition (Shklovski and Efros, 1979; Stauffer, 1985). Initially it was suggested as a method of descriptive statistics in cosmology by one of the authors (Shandarin, 1983b) and later it was developed and used in a series of papers (Zeldovich *et al.*, 1982; Bhavsar and Barrow, 1983; Melott *et al.*, 1983; Shandarin and Zeldovich, 1983; Einasto *et al.*, 1984; Dekel and West, 1985; Klypin, 1987).

Previously in Sec. III.D we mentioned the application of the percolation method to an analysis of continuous distributions (say, density ρ). Choosing some level ρ_c one can divide the whole volume onto regions of two kinds, "dense" with $\rho > \rho_c$ and "rarefied" with $\rho < \rho_c$. Then the fractions of volume as well as of mass contained in one of the components at two percolation thresholds can be used as the quantitative parameters characterizing topological properties of non-Gaussian random fields.

Astronomy of course gives us discrete distributions of galaxies in space. One could smooth out the pointlike galaxy distribution by means of a Gaussian "smoothing" window $e^{-r^2/2r_0^2}$ or something similar and afterwards use the continuous distributions. But there is a direct method for treating discrete distributions.

Let us begin with a discussion of an idealized system of particles (i.e., pointlike objects) in an infinite volume, assuming that the mean density of particles \bar{n} is finite.

Taking some radius r one can construct clusters of points according to two principles: (i) all particles separated by a distance less than r are "friends," and (ii) "the friend of my friend is my friend." Thus one can travel from any point of a chosen cluster to every other belonging to the same cluster, making several "leaps" (from point to point), each no longer than r . On the other hand to jump from one cluster to any other one has to make a "leap" longer than r . The number of particles in any given cluster may be arbitrary from 1 to ∞ .

Generally speaking at arbitrary r there are clusters consisting of various numbers of particles. The distribution of cluster populations may or may not include a cluster of infinite numbers of particles depending on r . At some critical value r_c a transition takes place from a distribution without an infinite cluster to that with an infinite cluster. This transition is commonly referred to as "percolation." At $r < r_c$ percolation does not occur,

whereas at $r > r_c$ it does. Instead of the dimensional parameter r , a dimensionless parameter

$$B = \frac{4}{3}\pi r^3 \bar{n} \tag{9.10}$$

is generally used in percolation theory. It has a transparent interpretation as the mean number of particles in a sphere of radius r .

It seems surprising that the critical value of the percolation parameter has not been calculated analytically even for a Poisson distribution of particles. It was estimated numerically for a finite number of particles ($N_t \sim 1000-4000$) in a cubical volume (Skal, Shklovski, and Efros, 1973) to be

$$B_c^{(P)} \approx 2.7. \tag{9.11}$$

We note that $B_c^{(P)}$ depends on the dimensionality of the space. In 2D it is about 4. One can easily infer that in 1D the term "percolation" has no sense, at least for a Poisson distribution of particles, since there are gaps between points of any sizes with small but finite probability.

Now let us go back to 3D. It is quite natural to suppose that if the particles tend to cluster around some lines or surfaces forming, respectively, a connected network or cellular structure, then the percolation parameter B_c would be less than that for a Poisson distribution $B_c^{(P)}$. On the other hand, if the particles tend to cluster in separated clumps, then $B_c > B_c^{(P)}$. The situation would be more complicated if both tendencies were present. However, in any case the inequality $B_c < B_c^{(P)}$ can be considered as a manifestation of the presence of a network structure in the particle distribution.

How to estimate B_c using existing samples of galaxies poses a practical problem. Originally a very simple technique was used (Shandarin, 1983b; Einasto *et al.*, 1984).

A sample of galaxies was studied in a region of cubic shape, and the percolation parameter B_c was estimated when the diameter of the largest cluster reached the size of the cube. However, most galaxy samples are carried out in conelike regions where this simple technique fails (Bhavsar and Barrow, 1983). Dekel and West (1985) also mentioned the dependence of the percolation parameter B_c on the number of galaxies in the sample.

The first problem can be solved by using a more elaborate technique to estimate B_c (Klypin, 1987). Klypin suggested using a known approximate asymptotic formula for growth of the mass (i.e., the number of particles, since they may be treated as identical) of the infinite cluster (in practice of course the mass of the largest one) at the percolation threshold $B = B_c + \delta B$. Another useful parameter is the mean mass of all clusters except the largest one. Its asymptotic behavior is also approximately known. It turned out that these parameters are less sensitive to the shape of the sample volume. In fact they are complementary, since one of them uses information about the largest cluster and the other one about all clusters except the largest one. The results obtained by Klypin shown in Table I generally confirm the earlier conclusions of Shandarin (1983b) and Einasto *et al.* (1984).

There is definite evidence for the existence of large-scale structure in the galaxy distribution, resembling a network of filaments or even an irregular cellular structure, which is in agreement with the visual impression. We infer this conclusion basically from the fact that B_c for the galaxy distributions is significantly less than $B_c^{(P)} \approx 2.7$, in spite of the rather large dispersion of B_c for different samples and even for the same sample analyzed by different methods.

The simulated samples (A) and (I) are given to illustrate the idea of using the percolation parameter B_c as a

TABLE I. The critical percolation parameter $B_c = \frac{4}{3}\pi r_c^3 \bar{n}$ estimated by different methods for observational and simulated distributions (Klypin, 1987). (0) is the catalog of galaxies with $M \leq -19.5$ (Einasto *et al.*, 1984); (G80) and (G160) are catalogs of galaxies of different depths ($80h_{50}^{-1}$ and $160h_{50}^{-1}$ Mpc). (A) is a simulated catalog (adiabatic fluctuations with hot dense matter). (I) is a simulated catalog (isothermal fluctuations) (Dekel and West, 1985). (C0) and (C1) are catalogs of clusters of galaxies (richness class $R \geq 0$ and $R \geq 1$, respectively).

Catalog	0	G80	G160	A	I	C0	C1
Objects	galaxies $M \leq -19.5$	galaxies $M \leq -18.5$	galaxies $M \leq -19.5$	points	points	clusters $R \geq 0$	clusters $R \geq 1$
Shape of region	cube	cone	cone	cube	sphere	cone	cone
Number of objects	866	576	1356	64^3	4000	190	110
B_c^a	L_{\max}	1.0	1.8	1.6	4	4.1	3.9
	M_{\max}		0.5	0.37	1.1	3.4	2.7
	$\langle M \rangle$		0.5	0.5;1.4;2.5	1.2	4.0	3.1

^aThe last three rows show the critical percolation parameter B_c estimated by using the length of the largest cluster (indicated as L_{\max}), or its mass (M_{\max}), and the mean mass of all clusters except the largest one ($\langle M \rangle$), respectively.

quantitative parameter sensitive to the topology of the density distributions.

Model (A) represents a "classical" example of network structure, while model (I) displays a clumpy distribution without noticeable connections between clumps.

It is interesting that the sample of clusters of galaxies displaying a similar power-law two-point correlation function [see Eqs. (9.7) and (9.9)] possesses different percolation properties from those of the galaxy samples. However, recently Tully (1987) found that in his sample of rich clusters percolation is attained more easily than in a Poisson distribution.

The dependence of B_c on N_l discussed by Dekel and West (1985) can be useful, since they found that it is different for different kinds of geometry (filaments, layers) dominant in the galaxy distribution (Shandarin and Zeldovich, 1986).

Not pretending to give a comprehensive review of statistical methods proposed to study large-scale galaxy distribution we mention also extensive analysis of the topology of large-scale structures (Gott *et al.*, 1987; Weinberg *et al.*, 1987; Melott *et al.*, 1988) and an attempt to measure the fractal dimensionality of large-scale structures (Jones *et al.*, 1988).

X. SUMMARY

At present the density distributions of different components constituting the mass of the universe may be characterized as intermittent.

A large fraction of baryonic matter (~ 0.5) is contained in stars occupying a total volume of only about 10^{-30} of the volume of the universe. Smoothed over the typical galaxy scale (~ 10 kpc $\approx 3 \times 10^{22}$ cm), the contrast in baryon density decreases considerably but still remains very high (the fraction of the total volume of galaxies amounts to no more than about 10^{-6}). The intermittent character still holds when the smoothing scale reaches the value of the mean galaxy separation (~ 5 Mpc), but the contrast in density falls to about 3–10. Smoothed over such a scale, the baryon density distribution could become similar to the density distribution of dark matter. If so, regions of high-density dark matter must have the shape of pancakes or filaments. Moreover, it is very likely that these objects form some kind of connected structure generally referred to as the network or cellular large-scale structure of the universe.

Actually the bulk of our information about large-scale structure is based on the study of the distribution of galaxies in space, and thus we come to the question: what degree of confidence do we have that the distribution of galaxies is similar to that of dark matter? Twenty years ago the reply would probably have been that galaxy distribution in space repeats the distribution of the total density. At present the problem does not seem simple at all. The admission that we have no clear ideas as to how the two distributions are related is now characterized by the term "biasing" (a tendency for clustering to be

stronger for one component). Probably all suggested types of biasing agree that galaxies formed in regions of high-density dark matter. However there are two possibilities: (a) Galaxies have a stronger tendency to cluster than does dark matter, or (b) vice versa.

In the HDM model galaxies form in pancakes only where the conditions are particularly favorable, primarily because the density is higher. However, outside pancakes the decrease in mass density hardly exceeds 10% of the mean value (Zeldovich and Shandarin, 1982a; Hoffman *et al.*, 1983; Melott, 1985) while the relative density of galaxies can be much less.

In the CDM model, galaxies arise before superclusters, but they have to do so inhomogeneously, otherwise the model would contradict the observations; in particular, the existence of huge voids between galaxies (Kirshner *et al.*, 1981). The model needs to invoke the hypothesis of biasing which, roughly speaking, states that galaxies form only in the peaks of total density. Numerical simulations including this hypothesis have shown a pretty good agreement between the simulated and observed large-scale structure (Davis *et al.*, 1985; White *et al.*, 1987). However, the question inevitably arises, what is the physical mechanism for this biasing? The problem has been addressed in several papers (Rees, 1985; Schaeffer and Silk, 1985; Silk, 1985; Dekel and Silk, 1986), but it would be premature to say that is solved (Peebles, 1986).

Another basic question is, what determines the present scale of the large-scale structure, i.e., the sizes of superclusters and voids? Does it occur as an effect of the nonlinear feedback due to release of nuclear energy in stars in the process of galaxy formation (Ostriker and Cowie, 1981) or was this scale somehow imprinted in the linear density fluctuations and the present large-scale structure is the manifestation of this scale?

The analysis presented above has shown that if the spectrum of density fluctuations in the linear approximation possesses a cutoff at short waves it results in the formation of filament structure at the beginning of the nonlinear stage. The steeper the cutoff, the more distinct the structure becomes. The crucial question of the nonlinear theory of gravitational instability is: what is the critical slope of the spectrum (assuming for simplicity that the spectrum obeys a power law) that separates the pancake scenario from hierarchical clustering?

The generally accepted answer to this question might be stated as follows: if the slope is steeper than $\delta_k^2 \propto k^{-3}$ at $k > k_c$, then the pancake scenario takes place; otherwise the hierarchical clustering picture is inevitable. The current nonlinear theory presented above gives a somewhat different answer. It states that pure hierarchical clustering takes place only if the spectrum falls off at short waves no steeper than $\delta_k^2 \propto k^{-1}$. In the intermediate range (i.e., $\delta_k^2 \propto k^n$ and $-3 < n < -1$), the nonlinear process of gravitational clustering possesses the features of both scenarios; it proceeds as a bottom-up sequence similar to hierarchical clustering, but large-scale perturbations influence the nonlinear evolution of much smaller

clumps, resulting in the formation of some kind of network structure analogous to the pancake picture. Probably for this reason power-law spectra $\delta_k^2 \propto k^n$ with spectral indices in the range $-3 < n < -1$ are the most difficult to analyze, both theoretically and numerically. However, in the (currently most popular) CDM model, this kind of spectrum is predicted in the range from galaxies to superclusters of galaxies.

In this review we have tried to call attention to the similarities between nonlinear gravitational instability in collisionless dark matter filling an expanding universe and nonlinear evolution of inhomogeneities of various kinds: brightness distribution in geometrical optics, collisionless noninteracting medium, and sticky dust. The nonlinear stage of gravitational instability possesses prominent features known as intermittency which are typical for various non-Gaussian random fields. These phenomena are well known in hydrodynamical and acoustic turbulence, nonlinear diffusion, and generation of magnetic fields (Barenblatt, 1978; Kravtsov and Orlov, 1983; Zeldovich *et al.*, 1987). These states of intermittency arise as a result of the nonlinear transformation of Gaussian random fields considered in synergetics; however, in the cases mentioned above, the role of initial conditions is much stronger.

In the Introduction two questions were asked: (i) what is the physical nature of the dark matter in the universe and (ii) what kinds of perturbations disturbed the perfect homogeneity of the universe at early stages?

At present there are no final answers to these questions. One of the most promising ways to solve these problems is to study the large-scale structure of the universe, which probably arises as a result of nonlinear gravitational instability.

ACKNOWLEDGMENTS

The authors express their gratitude to V. I. Arnold, G. I. Barenblatt, A. G. Doroshkevich, S. I. Gurbatov, A. A. Klypin, S. A. Molchanov, A. A. Ruzmaikin, A. I. Saichev, D. D. Sokolov, R. A. Sunyaev, A. S. Szalay, and many others for the discussions of various questions related to the subject of this review. S.F.S., who prepared the final version of the review during a two-month visit to the Max-Planck-Institute für Astrophysik in Garching, December 1987–January 1988, would like to thank Gerhard Börner, Thomas Buchert, Robert Klaffl, and other colleagues at the MPA for discussions, and especially Ronald Kates for kindly reading the manuscript and for conversations that both clarified the discussion of many questions in the review and improved the English. Thanks, as well, are due to Fräulein Petra Berkemeyer for typing of the manuscript. Finally, S.F.S. is deeply grateful to A. L. Melott and J. Primack for their criticism and useful suggestions.

REFERENCES

Aarseth, S. J., J. R. Gott III, and E. L. Turner, 1979, *Astrophys. J.* **228**, 664.

- Arnold, V. I., 1972, *Funct. Anal. Appl.* **6**, 254.
 Arnold, V. I., 1982, *Trudy Sem. Petrovskogo* **8**, 21 (in Russian).
 Arnold, V. I., 1986 *Catastrophe Theory* (Springer, Berlin/Heidelberg).
 Arnold, V. I., S. F. Shandarin, and Ya. B. Zeldovich, 1982, *Geophys. Astrophys. Fluid Dyn.* **20**, 111.
 Arnold, V. I., S. M. Gusein-Zade, and A. N. Varchenko, 1985, Eds., *Singularities of Differentiable Maps* (Birkhauser Boston, Cambridge, Massachusetts).
 Bahcall, N. A., and R. M. Soneira, 1983, *Astrophys. J.* **270**, 20.
 Bahcall, N. A., R. M. Soneira, and W. S. Barger, 1986, *Astrophys. J.* **311**, 15.
 Baranova, N. B., A. V. Mamaev, N. F. Pilipetsky, V. V. Shkunov, and B. Ya. Zeldovich, 1983, *J. Opt. Soc. Am.* **73**, 525.
 Bardeen, J. M., J. R. Bond, N. Kaiser, and A. S. Szalay, 1986, *Astrophys. J.* **304**, 15.
 Barenblatt, G. I., 1978, *Similarity and Intermediate Asymptotics* (Hydro. Meteorol. Press, Moscow), in Russian.
 Barnes, J., A. Dekel, G. Efstathiou, and C. Frenk, 1985, *Astrophys. J.* **295**, 368.
 Batuski, D. J., and J. O. Burns, 1985, *Astrophys. J.* **299**, 5.
 Bhavsar, S. P., and J. D. Barrow, 1983, *Mon. Not. R. Astron. Soc.* **205**, 61p.
 Bisnovaty-Kogan, G. S., and I. D. Novikov, 1980, *Astron. Zh.* **57**, 899 [*Sov. Astron.* **24**, 516 (1980)].
 Blumenthal, G. R., S. M. Faber, J. R. Primack, and M. J. Rees, 1984, *Nature (London)* **311**, 517.
 Blumenthal, G. R., and J. Primack, 1983, in *Fourth Workshop on Grand Unification*, edited by H. A. Weldon, P. Langacker, and P. J. Steinhardt (Birkhauser Boston, Cambridge, Massachusetts), p. 256.
 Bond, J. R., J. Centrella, A. S. Szalay, and J. R. Wilson, 1984, *Mon. Not. R. Astron. Soc.* **210**, 515.
 Bond, J. R., and G. Efstathiou, 1984, *Astrophys. J. Lett.* **285**, L45.
 Bond, J. R., and G. Efstathiou, 1987, *Mon. Not. R. Astron. Soc.* **226**, 655.
 Bond, J. R., and A. S. Szalay, 1983, *Astrophys. J.* **274**, 443.
 Bond, J. R., A. S. Szalay, and S. D. M. White, 1983, *Nature (London)* **301**, 584.
 Bonnor, W. B., 1957, *Mon. Not. R. Astron. Soc.* **117**, 104.
 Bouchet, F. R., J. A. Adam, and R. Pellat, 1985, *Astron. Astrophys.* **141**, 413.
 Buchert, T., 1988, unpublished.
 Burgers, J. M., 1948, *Adv. Appl. Mech.* **1**, 171.
 Burgers, J. M., 1974, *The Nonlinear Diffusion Equation* (Reidel, Dordrecht/Boston).
 Carnevali, P., A. Cavaliere, and P. Santangelo, 1981, *Astrophys. J.* **249**, 449.
 Carr, B. J., and S. Ikeuchi, 1985, *Mon. Not. R. Astron. Soc.* **213**, 497.
 Centrella, J., and A. L. Melott, 1983, *Nature (London)* **305**, 196.
 Centrella, J. M., J. S. Gallagher, A. L. Melott, and H. A. Bus-house, 1988, *Astrophys. J.* **333**, 24.
 Coles, P., 1986, *Mon. Not. R. Astron. Soc.* **222**, 9p.
 Couchman, H. M. P., 1987, *Mon. Not. R. Astron. Soc.* **225**, 777.
 Cowsik, R., and J. McClelland, 1973, *Astrophys. J.* **180**, 7.
 Davis, M. G., 1987, private communication.
 Davis, M. G., G. Efstathiou, C. Frenk, and S. D. M. White, 1985, *Astrophys. J.* **292**, 371.
 Davis, M. G., and P. J. E. Peebles, 1983, *Astrophys. J.* **267**, 465.
 Dekel, A., 1983, *Astrophys. J.* **264**, 373.
 Dekel, A., 1984, *Astrophys. J.* **284**, 445.

- Dekel, A., 1985, *Astrophys. J.* **298**, 461.
- Dekel, A., and S. J. Aarseth, 1984, *Astrophys. J.* **283**, 1.
- Dekel, A., and J. Silk, 1986, *Astrophys. J.* **303**, 39.
- Dekel, A., and M. J. West, 1985, *Astrophys. J.* **288**, 411.
- de Lapparent V., M. J. Geller, and J. P. Huchra, 1986, *Astrophys. J.* **302**, L1.
- Doroshkevich, A. G., 1970, *Astrophys.* **6**, 320.
- Doroshkevich, A. G., 1984, private communication.
- Doroshkevich A. G., and M. Yu. Khlopov, 1984, *Mon. Not. R. Astron. Soc.* **211**, 277.
- Doroshkevich, A. G., M. Yu. Khlopov, R. A. Sunyaev, A. S. Szalay, and Ya. B. Zeldovich, 1981 in *Proceedings of the Tenth Texas Symposium on Relativistic Astrophysics*, edited by R. Ramaty and F. C. Jones, *Annals of the New York Academy of Sciences* Vol. 375 (New York Academy of Sciences, New York), p. 32.
- Doroshkevich, A. G., E. V. Kotok, I. D. Novikov, A. N. Polyudov, S. F. Shandarin, and Yu. S. Sigov, 1980, *Mon. Not. R. Astron. Soc.* **192**, 321.
- Doroshkevich, A. G., V. S. Ryabenskii, and S. F. Shandarin, 1973, *Astrophysics* **9**, 144.
- Doroshkevich, A. G., and S. F. Shandarin, 1973, *Astrophysics* **9**, 332.
- Doroshkevich, A. G., and S. F. Shandarin, 1974, *Astron. Zh.* **51**, 41 [*Sov. Astron.* **18**, 24 (1974)].
- Doroshkevich, A. G., and Ya. B. Zeldovich, 1964, *Astron. Zh.* **40**, 807 [*Sov. Astron.* **7**, 615 (1964)].
- Doroshkevich, A. G., and Ya. B. Zeldovich, 1975, *Astrophys. Space Sci.* **35**, 55.
- Doroshkevich, A. G., Ya. B. Zeldovich, and R. A. Sunyaev, 1976, in *Origin and Evolution of Galaxies and Stars*, edited by S.B. Pikelner (Nauka, Moscow), p. 77 (in Russian).
- Eastwood, J. W., 1976, in *Computational Methods in Classical and Quantum Physics*, edited by M. B. Hooper (Advance Publications Limited/Hemisphere, Washington, D.C.), p. 196.
- Eckmann, J. P., 1981, *Rev. Mod. Phys.* **53**, 643.
- Efstathiou, G., 1979, *Mon. Not. R. Astron. Soc.* **187**, 117.
- Efstathiou, G., M. Davis, C. S. Frenk, and S. D. M. White, 1985, *Astrophys. J. Suppl.* **57**, 241.
- Efstathiou, G., and J. W. Eastwood, 1981, *Mon. Not. R. Astron. Soc.* **194**, 503.
- Efstathiou, G., M. S. Fall, and C. Hogan, 1979, *Mon. Not. R. Astron. Soc.* **189**, 203.
- Efstathiou, G., and J. Silk, 1983 *Fundam. Cosmic Phys.* **9**, 1.
- Einasto, J., M. Jeeveer, and E. Saar, 1987, in *Dark Matter in the Universe*, edited by J. Kormendy and G. R. Knapp (Reidel, Dordrecht), p. 243.
- Einasto, J., A. Klypin, and E. Saar, 1986, *Mon. Not. R. Astron. Soc.* **219**, 457.
- Einasto, J., A. A. Klypin, E. Saar, and S. F. Shandarin, 1984, *Mon. Not. R. Astron. Soc.* **206**, 529.
- Fall, M., 1978, *Mon. Not. R. Astron. Soc.* **185**, 165.
- Fall, M., 1979, *Rev. Mod. Phys.* **51**, 21.
- Fillmore, J. A., and P. Goldreich, 1984, *Astrophys. J.* **281**, 1.
- Frenk, C. S., S. D. M. White, and M. Davis, 1983, *Astrophys. J.* **271**, 417.
- Fridman, A., and V. Polyachenko, 1984, *Physics of Gravitating Systems* (Springer, Berlin).
- Gott, J. R., III, 1980, in *Physical Cosmology*, Les Houches Session XXXII, 1979, edited by R. Balian, Jean Audouze, and David N. Schramm (North-Holland, Amsterdam), p. 564.
- Gott, J. R., III, and M. J. Rees, 1975, *Astron. Astrophys.* **45**, 365.
- Gott, J. R., III, E. L. Turner, and S. J. Aarseth, 1979, *Astrophys. J.* **234**, 13.
- Gott, J. R., III, D. H. Weinberg, and A. L. Melott, 1987, *Astrophys. J.* **319**, 1.
- Grishcuk, L. P., and Ya. B. Zeldovich, 1981, *Astron. Zh.* **58**, 472 [*Sov. Astron.* **25**, 267 (1981)].
- Gurbatov, S. N., and A. I. Saichev, 1981, *Zh. Eksp. Teor. Fiz.* **80**, 689 [*Sov. Phys. JETP* **53**, 347 (1981)].
- Gurbatov, S. N., and A. I. Saichev, 1984, *Izv. Vyssh. Uchebn. Zaved. Radiofiz.* **27**, 456.
- Gurbatov, S. N., A. I. Saichev, and S. F. Shandarin, 1984, Institute of Applied Mathematics, Moscow, Preprint No. 152 (in Russian).
- Gurbatov, S. N., A. I. Saichev, and S. F. Shandarin, 1985, *Sov. Phys. Dokl.* **30**, 921.
- Gurbatov, S. N., A. I. Saichev, and S. F. Shandarin, 1989, *Mon. Not. R. Astron. Soc.*, in press.
- Guth, A., 1981, *Phys. Rev. D* **23**, 347.
- Guyot, M., and Ya. B. Zeldovich, 1970, *Astron. Astrophys.* **9**, 227.
- Hansel, D., F. R. Bouchet, R. Pellat, and A. Ramani, 1985, *Phys. Rev. Lett.* **55**, 437.
- Harrison, E. R., 1970, *Phys. Rev. D* **1**, 2726.
- Hauser, M. G., and P. J. E. Peebles, 1973, *Astrophys. J.* **185**, 757.
- Hoffman, G. L., E. E. Salpeter, and I. Wasserman, 1983, *Astrophys. J.* **268**, 527.
- Icke, V., and R. van de Weygaert, 1987, *Astron. Astrophys.* **184**, 16.
- Jones, B. J. T., V. J. Martinez, E. Saar, and J. Einasto, 1988, *Astrophys. J. Lett.* **332**, L1.
- Kaiser, N., 1984, *Astrophys. J.* **284**, L9.
- Kibble, T., 1976, *J. Phys. A* **9**, 1387.
- Kirshner, R. R., A. Oemier, P. L. Shechter, and S. A. Shechtman, 1981, *Astrophys. J.* **248**, L57.
- Klypin, A. A., 1987, *Sov. Astron.* **31**, 8.
- Klypin, A. A., and A. I. Kopylov, 1983, *Pis'ma Astron. Zh.* **9**, 75 [*Sov. Astron. Lett.* **9**, 41 (1983)].
- Klypin, A. A., and S. F. Shandarin, 1981, Institute of Applied Mathematics, Academy of Science USSR, Preprint No. 136 (in Russian) [*Mon. Not. R. Astron. Soc.* **204**, 891 (1983)].
- Kofman, L. A., and A. D. Linde, 1987, *Nucl. Phys. B* **282**, 555.
- Kofman, L. A., and S. F. Shandarin, 1988, *Nature (London)* **334**, 129.
- Kofman L., D. Pogossyan, and S. Shandarin, 1989, unpublished.
- Kopylov, A. I., D. Yu. Kuznetsov, T. S. Fetisova, and V. F. Shvartsman, 1984, *Astron. Tsirk. No.* 1347, 1 (in Russian); English translation appeared in *Large Scale Structures of the Universe*, edited by J. Audouze, M. Ch. Peletan, and A. Szalay (Kluwer Academic, Dordrecht, 1988), p. 129.
- Kotok, E. V., and S. F. Shandarin, 1987, *Sov. Astron.* **31**, 600.
- Kotok, E. V., and S. F. Shandarin, 1988, *Sov. Astron.*, in press.
- Kravtsov, Yu. A., and Yu. I. Orlov, 1983, *Usp. Fiz. Nauk* **141**, 591 [*Sov. Phys. Usp.* **26**, 1038 (1983)].
- Kuznetsov, N. N., and B. L. Rozhdestvensky, 1961, *Zh. Vychisl. Mat. Mat. Fiz.* **1**, 217.
- Lifshitz, E. M., 1946, *J. Phys. USSR Acad. Sci.* **10**, 116.
- Lifshitz, E. M., and I. M. Khalatnikov, 1963, *Sov. Phys. Usp.* **6**, 522.
- Linde, A., 1982, *Phys. Lett. B* **108**, 389.
- Linde, A. D., 1984, *Rep. Prog. Phys.* **47**, 925.
- Marx, G., and A. S. Szalay, 1972, in *Proceedings Neutrino 72* (Technoinform, Budapest), p. 123.
- McGlynn, T. A., and A. C. Fabian, 1984, *Mon. Not. R. Astron. Soc.* **208**, 709.

- Melchiorri, F., G. Moreno, G. Dall'Oglio, and B. Melchiorri, 1986, in *Cosmology, Astronomy and Fundamental Physics*, edited by G. Setti and L. Van Hove (European Southern Observatory, Garching bei München), p. 89.
- Melott, A. L., 1982a, *Phys. Rev. Lett.* **48**, 894.
- Melott, A. L., 1982b, *Nature (London)* **296**, 721.
- Melott, A. L., 1983a, *Astrophys. J.* **264**, 59.
- Melott, A. L., 1983b, *Mon. Not. R. Astron. Soc.* **202**, 595.
- Melott, A. L., 1985, *Astrophys. J.* **289**, 2.
- Melott, A. L., 1986, *Phys. Rev. Lett.* **56**, 1992.
- Melott, A. L., J. Einasto, E. Saar, I. Suisalu, A. A. Klypin, and S. F. Shandarin, 1983, *Phys. Rev. Lett.* **51**, 935.
- Melott, A. L., and R. J. Scherrer, 1987, *Nature (London)* **328**, 691.
- Melott, A. L., D. W. Weinberg, and J. R. Gott, 1988, *Astrophys. J.* **328**, 50.
- Menshikov, M. V., S. A. Molchanov, and A. F. Sidorenko, 1986, *Itogi Nauki Tekh. Teor. Veroyatnostey*, 53.
- Meszaros, P., 1974, *Astron. Astrophys.* **37**, 225.
- Miller, R. H., 1983, in *Early Evolution of the Universe and Its Present Structure*, edited by G. O. Abell and G. Chincarini (Reidel, Dordrecht), p. 411.
- Olive, K. A., D. N. Schramm, G. Steigmann, M. Turner, and J. Yang, 1981, *Astrophys. J.* **246**, 557.
- Oort, J. H., 1983, *Annu. Rev. Astron. Astrophys.* **21**, 373.
- Ostriker, J., and L. Cowie, 1981, *Astrophys. J.* **243**, L127.
- Ott, E., 1981, *Rev. Mod. Phys.* **53**, 655.
- Peacock, J. A., and A. F. Heavens, 1985, *Mon. Not. R. Astron. Soc.* **217**, 805.
- Peebles, P. J. E., 1968, *Astrophys. J.* **153**, 1.
- Peebles, P. J. E., 1980, *The Large Scale Structure of the Universe* (Princeton University, Princeton).
- Peebles, P. J. E., 1982a, *Astrophys. J.* **258**, 415.
- Peebles, P. J. E., 1982b, *Astrophys. J.* **263**, L1.
- Peebles, P. J. E., 1984a, *Astrophys. J.* **277**, 470.
- Peebles, P. J. E., 1984b, *Astrophys. J.* **284**, 439.
- Peebles, P. J. E., 1986, *Nature (London)* **321**, 27.
- Polnarev, A. G., and M. Yu. Khlopov, 1985, *Sov. Phys. Usp.* **28**, 273.
- Postman, M., J. P. Huchra, and M. J. Geller, 1986, *Astron. J.* **92**, 1238.
- Press, W. H., and P. Schechter, 1974, *Astrophys. J.* **187**, 425.
- Primack, J. R., 1986, in *Cosmology, Astronomy and Fundamental Physics*, edited by G. Setti and L. Van Hove (European Southern Observatory, Garching bei München), p. 193.
- Primack, J. R., and G. R. Blumenthal, 1984, in *Clusters and Groups of Galaxies*, edited by F. Mardirossian, G. Giuricin, and M. Mezzetti (Reidel, Dordrecht), p. 435.
- Rees, M., 1985, *Mon. Not. R. Astron. Soc.* **213**, p. 75.
- Rees, M., 1986, *Mon. Not. R. Astron. Soc.* **222**, p. 27.
- Roytvarf, A. A., 1987, *Vestnik Mosk. Univ.*, Ser. 1, No. 1, 65.
- Roytvarf, A. A., 1988, *Vestnik Mosk. Univ.*, Ser. 1, No. 3, 41.
- Rozhanskij, L. V., and S. F. Shandarin, 1984, *Institute of Applied Mathematics, Academy of Science USSR, Preprint No. 79* (in Russian).
- Saarinén, S., A. Dekel, and B. J. Carr, 1987, *Nature (London)* **325**, 598.
- Saichev, A. I., 1976, *Izv. Vyssh. Uchebn. Zaved. Radiofiz.* **19**, 418.
- Sakharov, A. D., 1965, *Zh. Eksp. Teor. Fiz.* **49**, 345 [*Sov. Phys. JETP* **22**, 241 (1966)].
- Sazhin, M. V., 1985, *Mon. Not. R. Astron. Soc.* **216**, p. 25.
- Schaeffer, R., and J. Silk, 1985, *Astrophys. J.* **292**, 319.
- Shandarin, S. F., 1983a, in *The Origin and Evolution of Galaxies*, edited by B. J. T. Jones and J. E. Jones (Reidel, Dordrecht), p. 171.
- Shandarin, S. F., 1983b, *Pis'ma Astron. Zh.* **9**, 195 [*Sov. Astron. Lett.* **9**, 104 (1983)].
- Shandarin, S. F., 1987, in *Dark Matter in the Universe*, edited by J. Kormendy and G. R. Knapp (Reidel, Dordrecht), p. 369.
- Shandarin, S. F., 1988, in *Large Scale Structures of the Universe*, edited by J. Audouze, M. Ch. Peletan, and A. Szalay (Kluwer Academic, Dordrecht), p. 273.
- Shandarin, S. F., A. G. Doroshkevich, and Ya. B. Zeldovich, 1983, *Usp. Fiz. Nauk* **139**, 83 [*Sov. Phys. Usp.* **26**, 46 (1983)].
- Shandarin, S. F., and A. A. Klypin, 1984, *Astron. Zh.* **61**, 837 [*Sov. Astron.* **28**, 491 (1984)].
- Shandarin, S. F., and Ya. B. Zeldovich, 1983, *Comments Astrophysics. Space Phys.* **10**, 33.
- Shandarin, S. F., and Ya. B. Zeldovich, 1984, *Phys. Rev. Lett.* **52**, 1488.
- Shandarin, S. F., and Ya. B. Zeldovich, 1986, in *Cosmology, Astronomy and Fundamental Physics*, edited by G. Setti and L. Van Hove (European Southern Observatory, Garching bei München), p. 45.
- Shapiro, P. R., C. Struck-Marcell, and A. L. Melott, 1983, *Astrophys. J.* **275**, 413.
- Shklovski, B. I., and A. L. Efros, 1979, *Electronic Properties of Alloyed Semiconductors* (Nauka, Moscow) (in Russian).
- Shukurov, A. M., 1981, *Astrophysics* **17**, 263.
- Silk, J., 1985, *Astrophys. J.* **297**, 1.
- Silk, J., A. S. Szalay, and Ya. B. Zeldovich, 1983, *Sci. Am.* **249**, No. 4, 72.
- Skal, A. S., B. I. Shklovski, and A. L. Efros, 1973, *Pis'ma Zh. Eksp. Teor. Fiz.* **17**, 522 [*JETP Lett.* **17**, 377 (1973)].
- Starobinsky, A. A., 1980, *Phys. Lett. B* **91**, 99.
- Starobinsky, A. A., and V. Sahni, 1984, in *Modern Theoretical and Experimental Problems of General Relativity* (Moscow), p. 77 (in Russian); English translation appeared in 1986 as Newcastle University Preprint No. NCL-TP12.
- Stauffer, D., 1985, *Introduction to Percolation Theory* (Taylor and Francis, Bristol).
- Sunyaev, R. A., and Ya. B. Zeldovich, 1972, *Astron. Astrophys.* **20**, 189.
- Szalay, A. S., and G. Marx, 1976, *Astron. Astrophys.* **49**, 437.
- Tago, E., J. Einasto, and E. Saar, 1986, *Mon. Not. R. Astron. Soc.* **218**, 177.
- Totsuji, H., and T. Kihara, 1969, *Publ. Astron. Soc. Jpn.* **21**, 221.
- Trimble, V., 1987, *Annu. Rev. Astron. Astrophys.* **25**, 425.
- Tully, R. B., 1987, *Astrophys. J.* **323**, 1.
- Turner, M., 1987, in *Dark Matter in the Universe*, edited by J. Kormendy and G. R. Knapp (Reidel, Dordrecht), p. 445.
- Turner, E. L., S. J. Aarseth, J. R. Gott III, N. T. Blanchard, and R. D. Mathien, 1979, *Astrophys. J.* **228**, 684.
- Turok, N., 1986, in *Cosmology, Astronomy and Fundamental Physics*, edited by G. Setti and L. Van Hove (European Southern Observatory, Garching bei München), p. 175.
- Vilenkin, A., 1981, *Phys. Rev. D* **23**, 852.
- Vilenkin, A., 1985, *Phys. Rep.* **121**, 263.
- Vittorio, N., and R. Juszkewicz, 1987, *Astrophys. J.* **314**, L29.
- Weinberg, D. H., J. Charlton, A. Dekel, J. R. Gott, A. L. Melott, J. Ostriker, and R. Scherrer, 1988, unpublished.
- Weinberg, D. H., J. R. Gott III, and A. L. Melott, 1987, *Astrophys. J.* **321**, 2.
- White, S. D. M., M. Davis, and C. S. Frenk, 1984, *Mon. Not. R. Astron. Soc.* **209**, p. 27.
- White, S. D. M., C. S. Frenk, and M. Davis, 1983, *Astrophys. J.*

- 274, L1.
- White, S. D. M., C. S. Frenk, M. Davis, and G. Efstathiou, 1987, *Astrophys. J.* **313**, 505.
- White, S. D. M., and M. J. Rees, 1978, *Mon. Not. R. Astron. Soc.* **183**, 341.
- Zabotin, N. A., and P. D. Naselskii, 1985, *Astron. Zh.* **62**, 1053 [*Sov. Astron.* **29**, 614 (1985)].
- Zeldovich, Ya. B., 1970, *Astron. Astrophys.* **5**, 84.
- Zeldovich, Ya. B., 1972, *Mon. Not. R. Astron. Soc.* **160**, 1p.
- Zeldovich, Ya. B., 1980, *Mon. Not. R. Astron. Soc.* **192**, 663.
- Zeldovich, Ya. B., 1982a, *Pis'ma Astron. Zh.* **8**, 195 [*Sov. Astron. Lett.* **8**, 102 (1982)].
- Zeldovich, Ya. B., 1982b, *Sov. Astron.* **59**, 636.
- Zeldovich, Ya. B., 1983, *Dok. Akad. Nauk SSSR* **270**, 1369 [*Sov. Phys. Dokl.* **28**, 490 (1983)].
- Zeldovich, Ya. B., 1984, in *Soviet Scientific Reviews, Sec. E, Astrophysics and Space Physics Reviews*, edited by R. A. Syunyaev (Harwood Academic, New York/London/Chur), Vol. 3, p. 1.
- Zeldovich, Ya. B., J. Einasto, and S. F. Shandarin, 1982, *Nature (London)* **300**, 407.
- Zeldovich, Ya. B., V. G. Kurt, and R. A. Syunyaev, 1968, *Zh. Eksp. Teor. Fiz.* **55**, 278 [*Sov. Phys. JETP* **28**, 146 (1969)].
- Zeldovich, Ya. B., A. V. Mamaev, and S. F. Shandarin, 1983, *Usp. Fiz. Nauk* **139**, 153 [*Sov. Phys. Usp.* **26**, 77 (1983)].
- Zeldovich, Ya. B., S. A. Molchanov, A. A. Ruzmaikin, and D. D. Sokolov, 1987, *Usp. Fiz. Nauk* **152**, 3 [*Sov. Phys. Usp.* **30**, 353 (1987)].
- Zeldovich, Ya. B., and I. D. Novikov, 1983, *The Structure and Evolution of the Universe* (University of Chicago, Chicago/London).
- Zeldovich, Ya. B., and S. F. Shandarin, 1982a, *Pis'ma Astron. Zh.* **8**, 131 [*Sov. Astron. Lett.* **8**, 67 (1982)].
- Zeldovich, Ya. B., and S. F. Shandarin, 1982b, *Pis'ma Astron. Zh.* **8**, 259 [*Sov. Astron. Lett.* **8**, 139 (1982)].
- Zwicky, F., 1933, *Helv. Phys. Acta* **6**, 110.

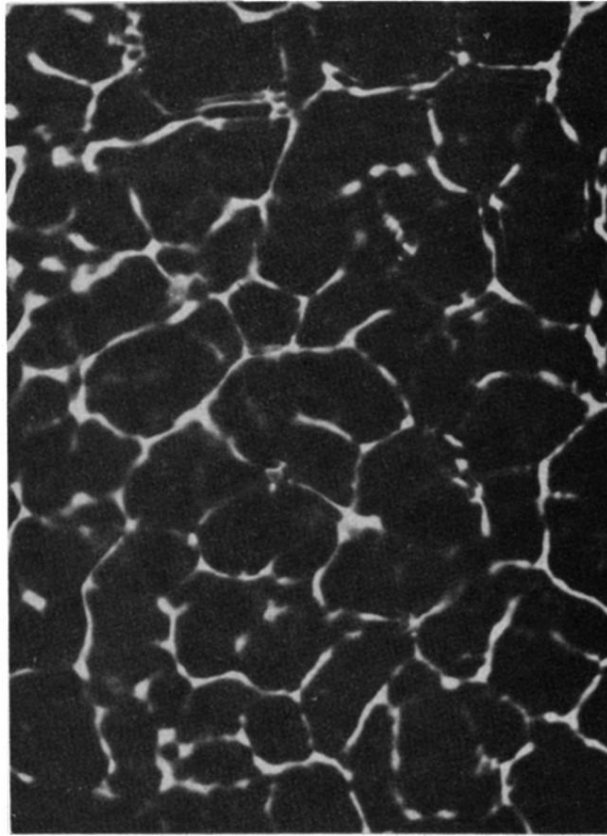
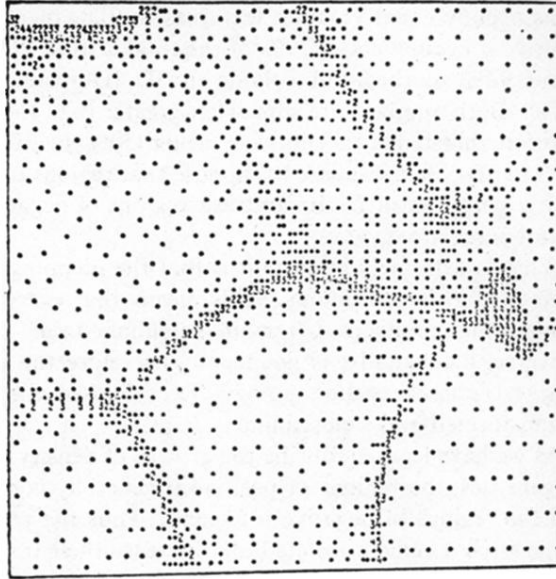


FIG. 11. Distribution of brightness on the screen in the optical experiment shown in Fig. 10.

(a)



(b)

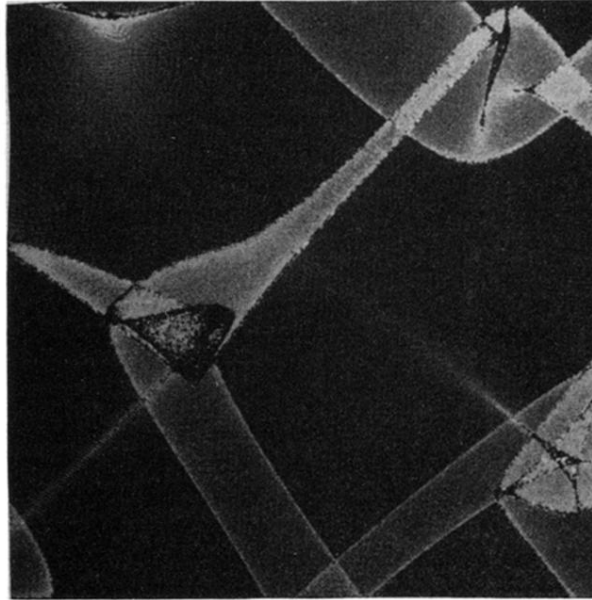


FIG. 12. Distribution of particle density at the early nonlinear stage in 2D: (a) poor resolution (Shandarin, 1975); (b) fine resolution (Buchert, 1988).